Supporting Information

Aluminum Complexes with New Non-Symmetric Ferrocenyl Amidine Ligands and their Application in CO_2 Transformation into Cyclic Carbonates

Yersica Rios Yepes,[a] *Javier Martínez,*[a] *Hiram Rangel Sánchez,*[b] *Celso Quintero,*[a] *M. Carmen Ortega-Alfaro,*[c] *José G. López Cortés,**[,b] *Constantin G. Daniliuc,*[d] *Antonio Antiñolo,*[e] *Alberto Ramos,*[e] *René S. Rojas**[,a]

[a]Laboratorio de Química Inorgánica, Facultad de Química Universidad Católica de Chile, Casilla 306, Santiago-22 6094411, Chile. E-mail: rrojasg@uc.cl

[b]Instituto de Química, Universidad Nacional Autónoma de México, Circuito Exterior, Cuidad Universitaria, Coyoacán, C.P. 04360 México D.F., México.

[c]Instituto de Ciencias Nucleares, Universidad Nacional Autónoma de México, Circuito Exterior, Cuidad Universitaria, Coyoacán, C.P. 04360 México D.F., México.

[d]Chemisches Institut der Universität Münster, Corrensstrasse 40, 48149 Münster, Germany.

[e]Centro de Innovación en Química Avanzada (ORFEO-CINQA), Departamento de Química Inorgánica, Orgánica y Bioquímica, Facultad de Ciencias y Tecnologías Químicas, Universidad de Castilla La Mancha, 13071 Ciudad Real, Spain

Table of Contents

1. Experimental Section

General procedure for the synthesis of cyclic carbonates at 1 bar pressure

An epoxide **5a–j** (1.7 mmol), catalysts **1** (28.9 μmol) and Bu_4NI (28.9 μmol) were placed in a sample vial with a magnetic stirrer bar. The sample vial was fitted with a rubber stopper pierced by a balloon filled with CO_2. The reaction mixture was stirred at 25 or 80 ºC for 24 or 48 h. The conversion of epoxide to cyclic carbonate was then determined by analysis of a sample by ^{1}H NMR spectroscopy relative to starting epoxide. The remaining sample was filtered through a plug of silica, eluting with CH_2Cl_2 to remove the catalyst. The eluent was evaporated in vacuo to give either the pure cyclic carbonate or a mixture of cyclic carbonate and unreacted epoxide. In the latter case, the mixture was purified by flash chromatography using a solvent system of first hexane, then hexane:EtOAc (9:1), then hexane:EtOAc (6:1) then hexane:EtOAc (3:1), then EtOAc to give the pure cyclic carbonate. Cyclic carbonates **6a–j** are all known compounds and the spectroscopic data for samples prepared using catalysts **1** were consistent with those reported in the literature.[1–8]

Electrochemical Measurements

All measurements were performed using a glovebox techniques under an atmosphere of dry nitrogen. Cyclic Voltammetric (CV) experiments were recorded with a portable Bipotentiostat/Galvanostat μStat 400 from Dropsens and scans rates from 25 to 500 mV/s were employed to assess the chemical and electrochemical reversibility of the observed redox transformations. The supporting electrolyte used was tetra-*n*-butylammonium hexafluroophosphate, *n*-Bu_4NPF_6 (Sigma Aldrich) for electrochemical analysis. The supporting electrolyte concentration was 2.0 M and was prepared according a reported method.[9] Solution were 10^{-3} M in the redox-active species. A conventional three-electrode cell was used. The counter and reference electrodes were a Pt wire, and a silver wire working electrode. Potential calibrations were performed in situ for all samples at the end of each data collection cycle by addition of 1 equiv of ferrocene per complex and the used of the ferrocenium/ferrocene couple as an internal reference.

X-ray crystal structure analyses

X-Ray diffraction: For compounds **1** and **3** data sets were collected with a Nonius Kappa CCD diffractometer. Programs used: data collection, COLLECT;[10] data reduction Denzo-SMN;[11] absorption correction, Denzo;[12] structure solution SHELXT-2015;[13] structure refinement SHELXL-2015.[14] *R*-values are given for observed reflections, and *w*R^2 values are given for all reflections. For compound **4** data sets were collected with a Bruker APEX II CCD diffractometer. Programs used: data collection:[15] APEX3 V2016.1-0 (Bruker AXS Inc., **2016**); cell refinement: SAINT V8.37A (Bruker AXS Inc., **2015**); data reduction: SAINT V8.37A (Bruker AXS Inc., **2015**); absorption correction, SADABS V2014/7 (Bruker AXS Inc., **2014**); structure solution SHELXT-2015;[13] structure refinement SHELXL-2015[14] and graphics, *XP* (Version 5.1, Bruker AXS Inc., Madison, Wisconsin, USA, **1998**).[16] *Exceptions and special features*: Compound **3** was refined as a 2-component twin using the 'HKLF 5' option, whereby the BASF factor was refined to 0.31. Crystallographic data for **1**, **3** and **4** have been deposited with Cambridge Crystallographic Data Centre, CCDC numbers for **1**, **3** and **4** are 1923169, 1923170 and 1923171, respectively. These data can be obtained free at www.ccdc.cam.ac.uk/data_request/cif [or from the Cambridge Crystallographic Data Centre, 12 Union Road, Cambridge CB2 1EZ, UK; fax: +44(1223)336-033, e- mail: deposit@ccdc.cam.ac.uk].

2. Structural Characterization for Ligands L_1H–L_2H and complexes 1–4

Ligand L_1H. (Yield: 83%, 541.16 mg). **^1H, ^{13}C-HMBC** (400 MHz / 100 MHz, DMSO-d_6, 298 K): $\delta(^1H) / \delta(^{13}C)$ = 7.04 / 146.49, 27.38 (H_9 / $C_{7,11}$), 6.91 / 137.66 (H_{10} / C_8), 4.76 / 62.98 (H_2 / C_3), 4.10 / 68.45 (H_4 / C_4), 3.91 / 99.32, 59.38 (H_3 / $C_{1,2}$), 3.00 / 146.49, 137.66, 122.45, 22.91, 23.61 (H_{11} / $C_{7,8,9,12,13}$), 1.58 / 151.91 (H_6 / C_5), 1.13 / 137.66, 27.38, 23.61 (H_{12} / $C_{8,11,13}$), 1.13 / 137.66, 27.38, 22.91 (H_{13} / $C_{8,11,12}$). **^1H, ^{13}C-HSQC** (400 MHz / 100 MHz, DMSO-d_6, 298 K): $\delta(^1H) / \delta(^{13}C)$ = 7.04 / 122.45 (H_9 / C_9), 6.91 / 121.65 (H_{10} / C_{10}), 4.76 / 59.38 (H_2 / C_2), 4.10 / 68.45 (H_4 / C_4), 3.91 / 62.98 (H_3 / C_3), 3.00 / 27.38 (H_{11} / C_{11}), 1.58 / 17.69 (H_6 / C_6), 1.13 / 22.91 (H_{12} / C_{12}), 1.13 / 23.61 (H_{13} / C_{13}). **^1H, ^1H-COSY** (400 MHz / 400 MHz, DMSO-d_6, 298 K): $\delta(^1H) / \delta(^1H)$ = 7.04 / 6.91 (H_9/ H_{10}), 4.76 / 3.91 (H_2 / H_3), 3.00 / 1.13, 1.13 (H_{11} / $H_{12,13}$).

Figure S1. ^1H NMR spectrum of ligand **L_1H** in DMSO-d_6

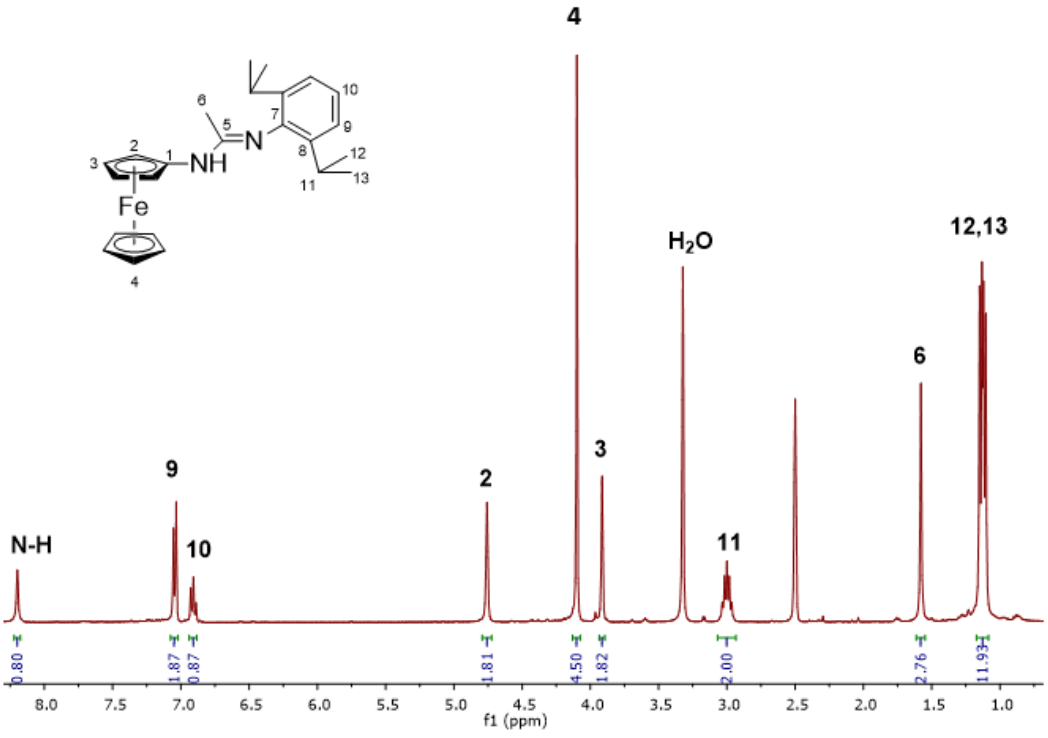

Figure S2. $^{13}C\{^{1}H\}$ NMR spectrum of ligand **L_1H** in DMSO-d_6

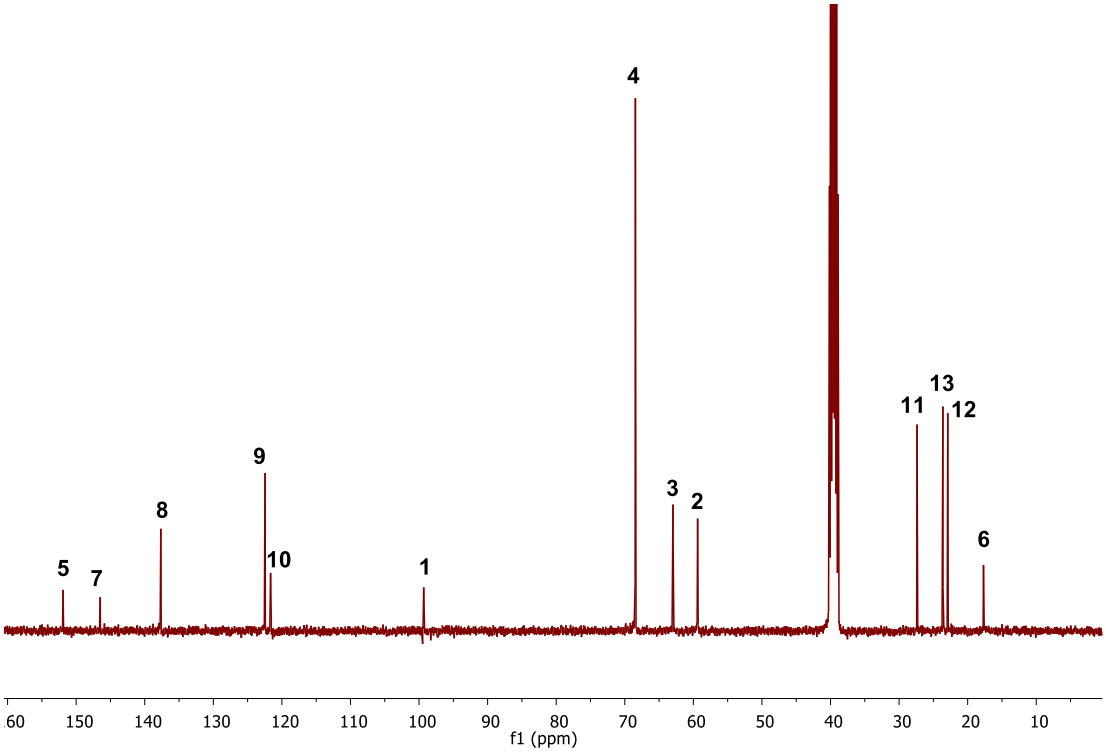

Figure S3. CVs at different scans rates of **L_1H** (10^{-3} M) recorded in CH_2Cl_2 containing 0.2 M of *n*-Bu_4NPF_6.

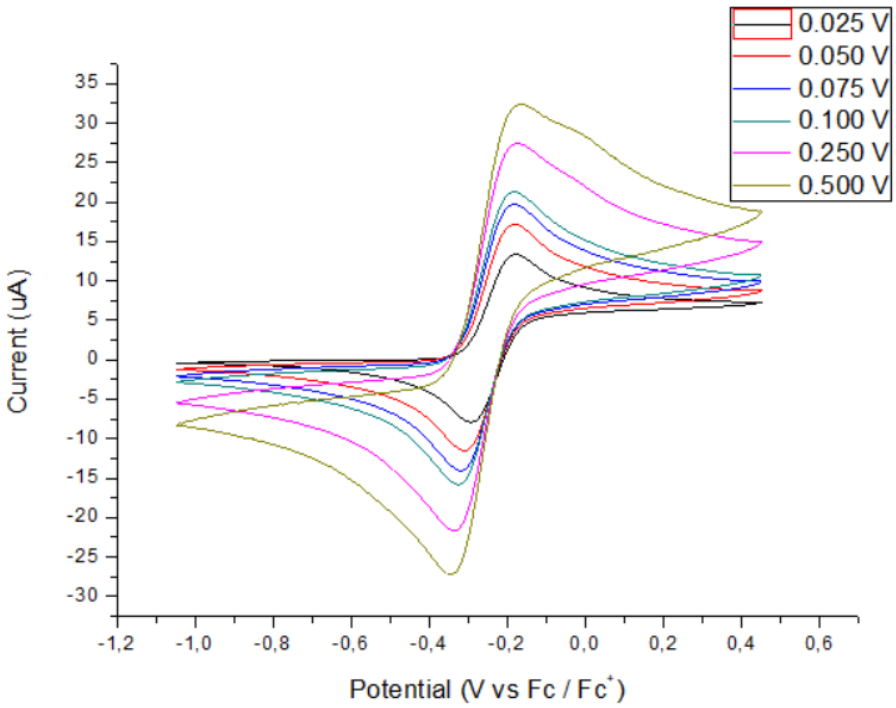

Ligand L_2H. (Yield: 71%, 1.22 g). **^{1}H, ^{13}C-HMBC** (400 MHz / 100 MHz, DMSO-d_6, 298 K): $\delta(^1H)$ / $\delta(^{13}C)$ = 8.15 / 151.96, 59.74 (NH / $C_{5,2}$), 6.98 / 127.38, 18.04 (H_9 / $C_{7,11}$), 6.75 / 149.35, 127.49 (H_{10} / $C_{8,9}$), 4.75 / 99.14, 63.01 (H_2 / $C_{1,3}$), 4.12 / 63.01 (H_4 / C_3), 3.91 / 99.14, 68.52, 59.74 (H_3 / $C_{1,4,2}$), 2.04 / 149.35, 127.38, 127.49 (H_{11} / $C_{8,7,9}$), 1.56 / 151.96 (H_6 / C_5). **^{1}H, ^{13}C-HSQC** (400 MHz / 100 MHz, DMSO-d_6, 298 K): $\delta(^1H)$ / $\delta(^{13}C)$ = 6.98 / 127.49 (H_9 / C_9), 6.75 / 120.84 (H_{10} / C_{10}), 4.75 / 59.74 (H_2 / C_2), 4.12 / 68.52 (H_4 / C_4), 3.91 / 63.01 (H_3 / C_3), 2.04 / 18.04 (H_{11} / C_{11}), 1.56 / 17.45 (H_6 / C_6). **^{1}H, ^{1}H-COSY** (400 MHz / 400 MHz, DMSO-d_6, 298 K): $\delta(^1H)$ / $\delta(^1H)$ = 6.98 / 6.75, 2.04 (H_9 / $H_{10,11}$), 4.75 / 3.91 (H_2 / H_3).

Figure S4. ^{1}H NMR spectrum of ligand **L_2H** in DMSO-d_6

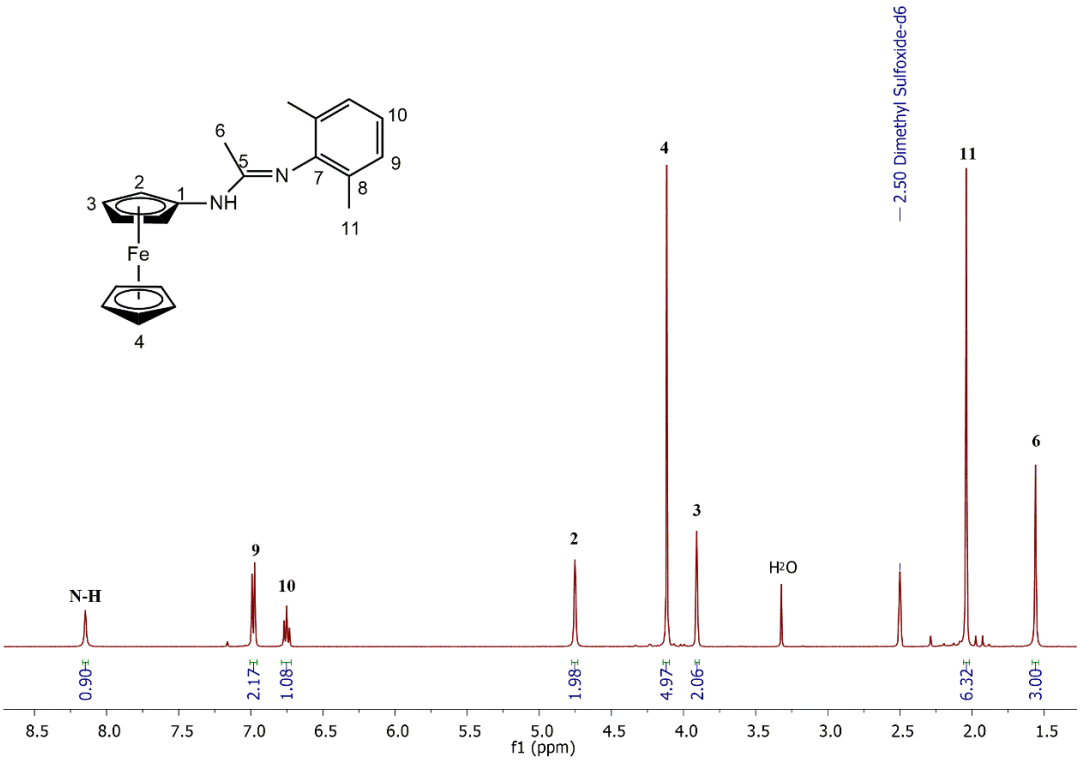

Figure S5. $^{13}C\{^{1}H\}$ NMR spectrum of ligand **L_2H** in DMSO-d_6

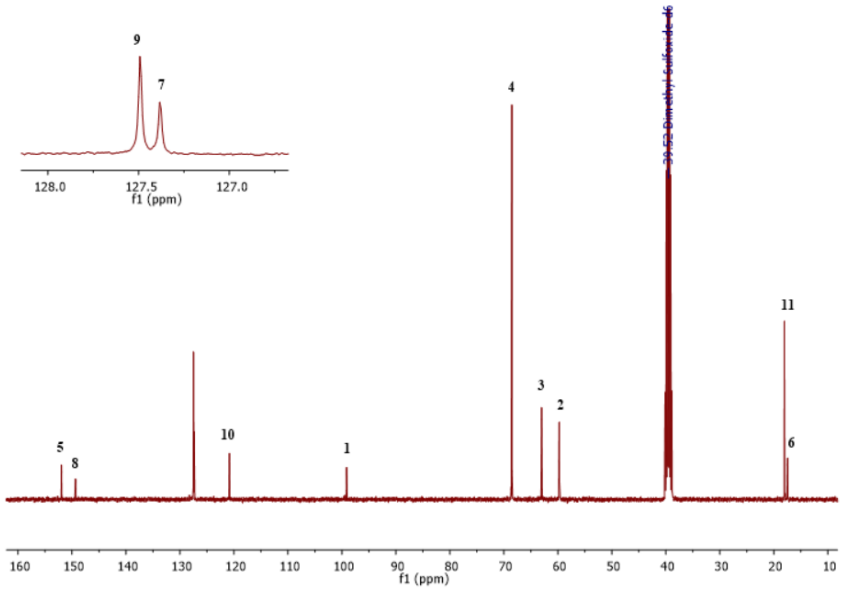

Figure S6. CVs at different scans rates of **L_2H** (10^{-3} M) recorded in CH_2Cl_2 containing 0.2 M of *n*-Bu_4NPF_6.

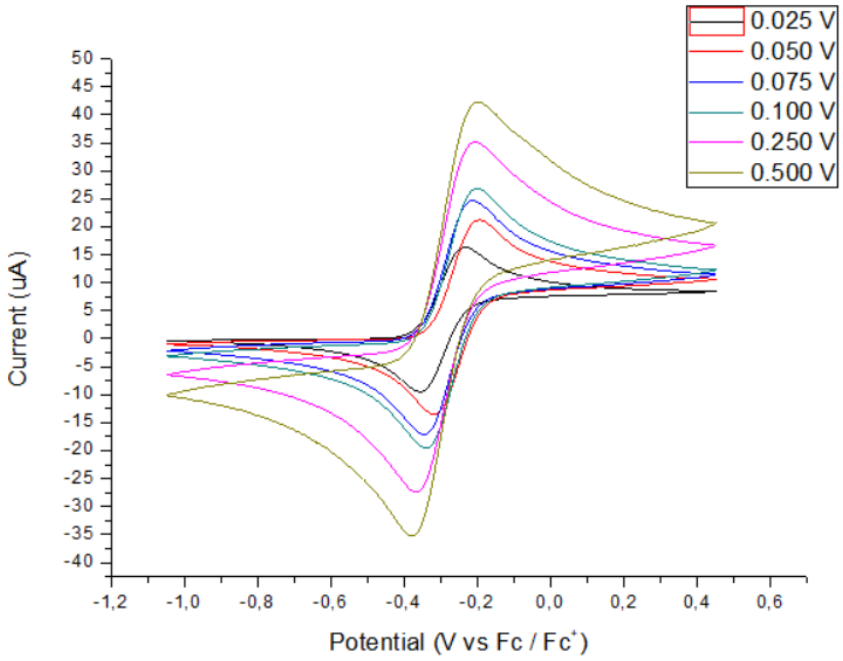

Aluminum complex 1, [(L_1)$AlMe_2$]. (Yield: 96%, 163 mg). **^{1}H, ^{13}C-HMBC** (400 MHz / 100 MHz, C_6D_6, 298 K): δ(^{1}H) / δ(^{13}C) = 7.14 / 144.85 (H_{10} / C_8), 7.08 / 138.09, 28.44 (H_9 / $C_{7,11}$), 4.01 / 65.19 (H_2 / C_3), 3.83 / 100.32, 63.09 (H_3 / $C_{1,2}$), 3.24 / 144.85, 138.09, 123.98, 24.71, 23.83 (H_{11} / $C_{8,7,9,12,13}$), 1.58 / 174.89 (H_6 / C_5), 1.18 / 144.85, 28.44, 23.83 (H_{12} / $C_{8,11,13}$), 1.10 / 144.85, 28.44, 24.71 (H_{13} / $C_{8,11,12}$). **^{1}H, ^{13}C-HSQC** (400 MHz / 100 MHz, C_6D_6, 298 K): δ(^{1}H) / δ(^{13}C) = 7.14 / 126.59 (H_{10} / C_{10}), 7.08 / 123.98 (H_9 / C_9), 4.13 / 69.40 (H_4 / C_4), 4.01 / 63.09 (H_2 / C_2), 3.83 / 65.19 (H_3 / C_3), 3.24 / 28.44 (H_{11} / C_{11}), 1.58 / 14.53 (H_6 / C_6), 1.18 / 24.71 (H_{12} / C_{12}), 1.10 / 23.83 (H_{13} / C_{13}), −0.11 / −9.42 (H_{14} / C_{14}). **^{1}H, ^{1}H-COSY** (400 MHz / 400 MHz, C_6D_6, 298 K): δ(^{1}H) / δ(^{1}H) = 7.14 / 7.08 (H_{10}/ H_9), 4.01 / 3.83 (H_2 / H_3), 3.24 / 1.18, 1.10 (H_{11} / $H_{12,13}$).

Figure S7. ^{1}H NMR spectrum of complex **1** in C_6D_6

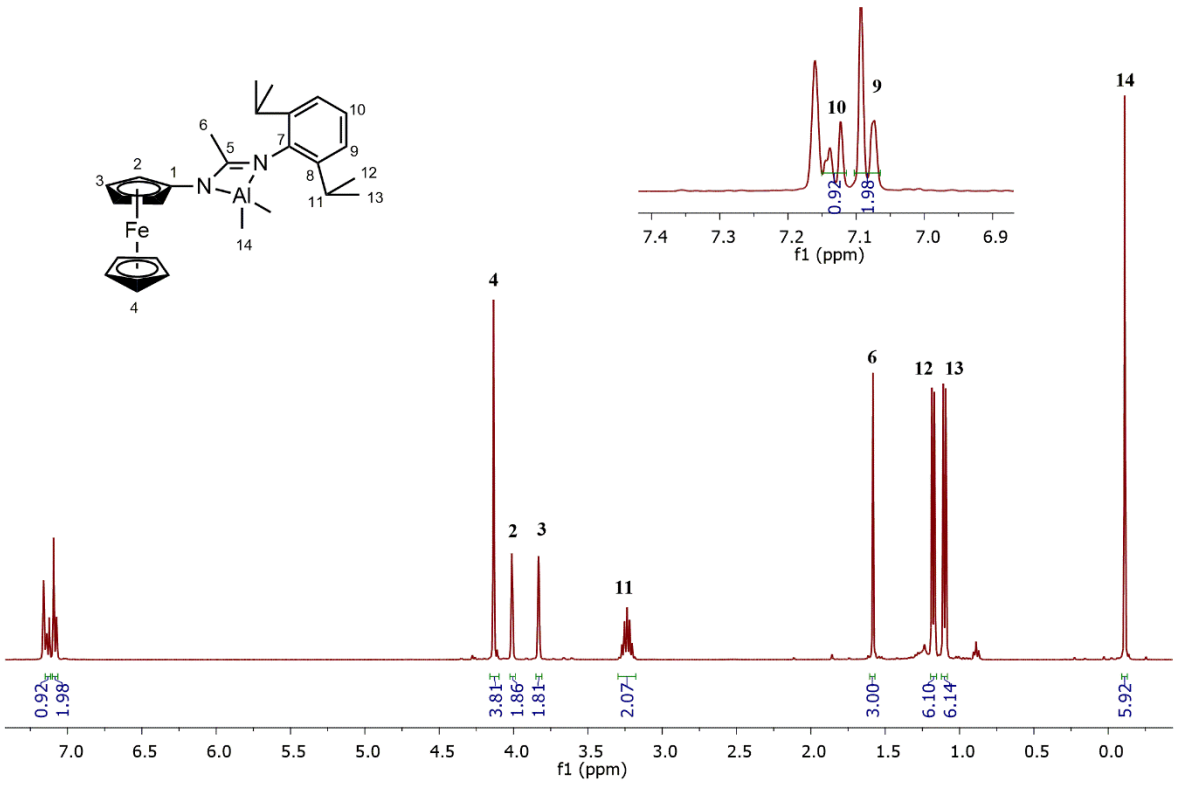

Figure S8. $^{13}C\{^{1}H\}$ NMR spectrum of complex **1** in C_6D_6

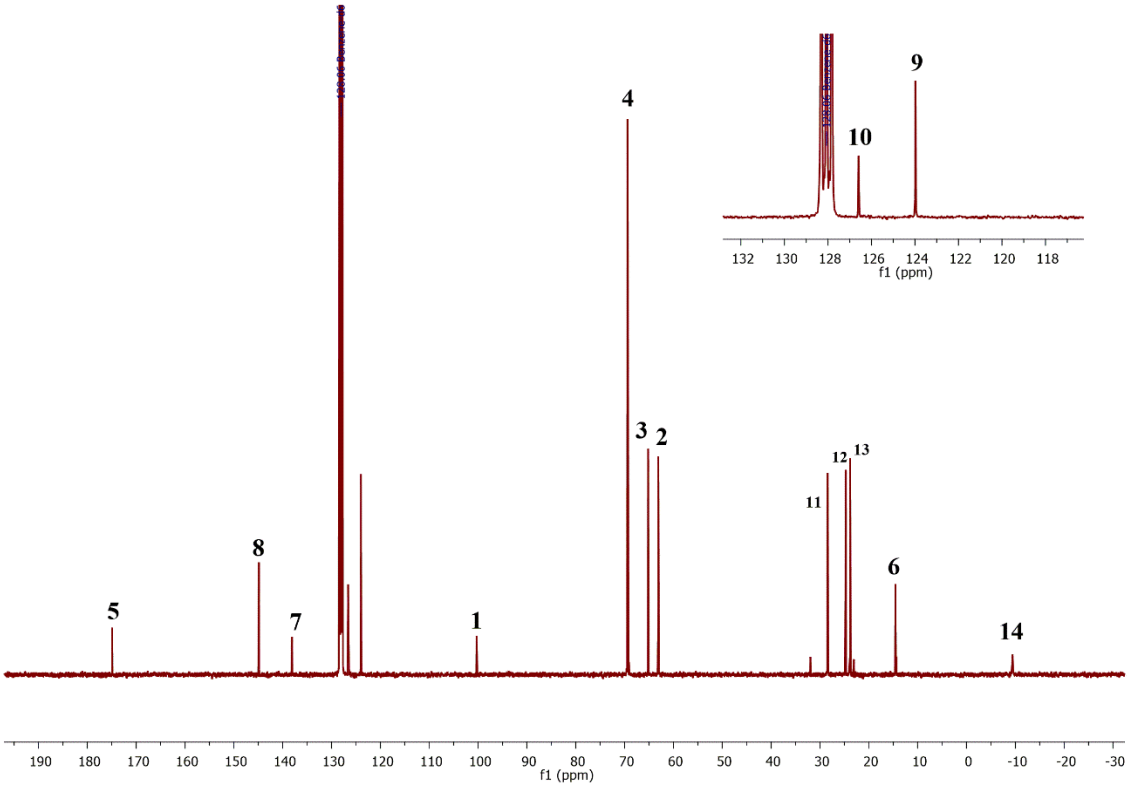

Figure S9. CVs at different scans rates of complex **1** (10^{-3} M) recorded in CH_2Cl_2 containing 0.2 M of *n*-Bu_4NPF_6.

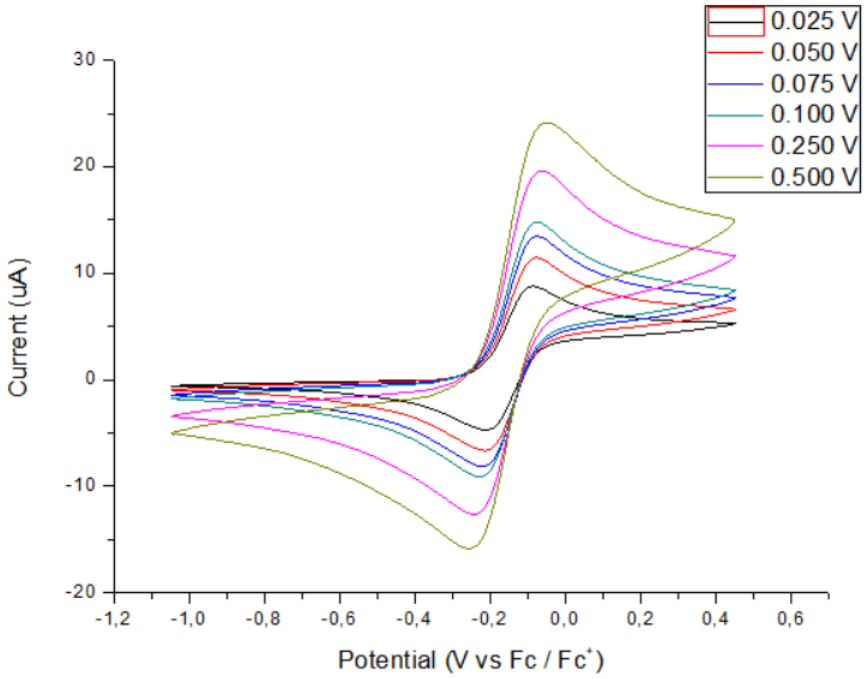

Figure S10. X ray crystal structure of complex 1. Thermal ellipsoids are shown with 15% probability. Hydrogen atoms were omitted for clarity

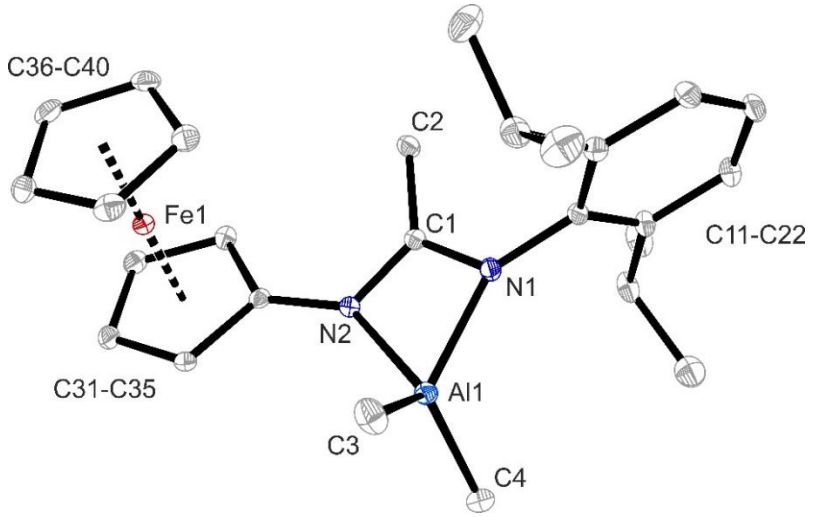

Aluminum complex 2, [(L$_2$)AlMe$_2$]. (Yield: 85%, 297.5 mg). **^{1}H, ^{13}C-HMBC** (400 MHz / 100 MHz, C_6D_6, 298 K): δ(^{1}H) / δ(^{13}C) = 6.97–6.94 / 141.42, 59.74 (H_{10} / C_8), 6.97–6.94 / 134.34, 18.86 (H_9 / $C_{7,11}$), 3.99 / 100.29, 65.16 (H_2 / $C_{1,3}$), 3.83 / 100.29, 63.15 (H_3 / $C_{1,2}$), 2.08 / 141.42, 134.34, 128.58 (H_{11} / $C_{8,7,9}$), 1.43 / 174.01 (H_6 / C_5). **^{1}H, ^{13}C-HSQC** (400 MHz / 100 MHz C_6D_6, 298 K): δ(^{1}H) / δ(^{13}C) = 6.97–6.94 / 125.56 (H_{10} / C_{10}), 6.97–6.94 / 128.58 (H_9 / C_9), 4.13 / 69.39 (H_4 / C_4), 3.99 / 63.15 (H_2 / C_2), 3.83 / 65.16 (H_3 / C_3), 2.08 / 18.86 (H_{11} / C_{11}), 1.43 / 13.69 (H_6 / C_6), −0.16 / −8.91 (H_{12} / C_{12}). **^{1}H, ^{1}H-COSY** (400 MHz / 400 MHz, C_6D_6, 298 K): δ(^{1}H) / δ(^{1}H) = 6.97–6.94 / 6.97–6.94 (H_{10} / H_9), 3.99 / 3.83 (H_2 / H_3).

Figure S11. ^{1}H NMR spectrum of complex **2** in C_6D_6

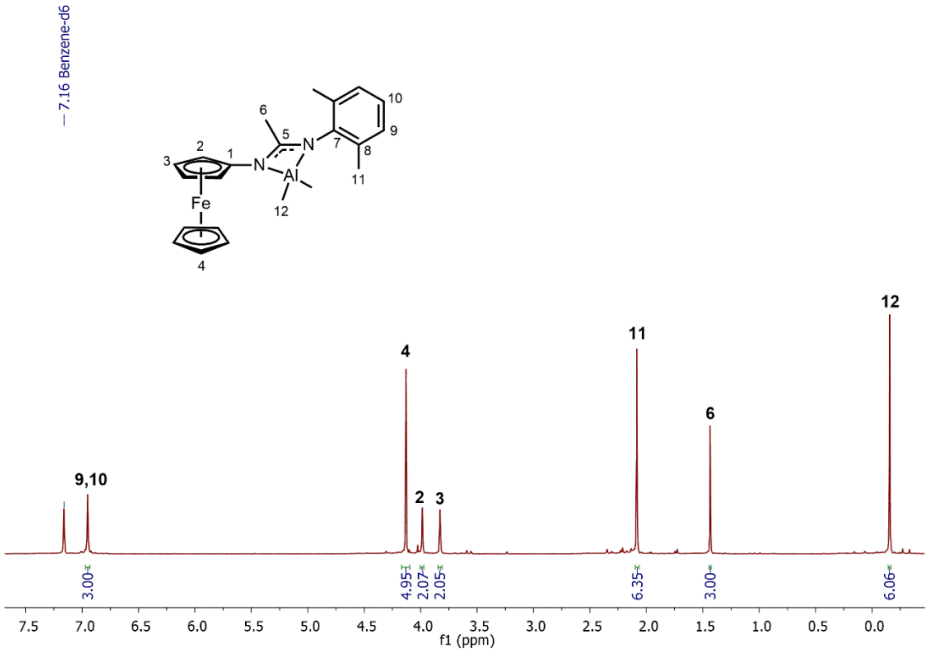

Figure S12. $^{13}C\{^{1}H\}$ NMR spectrum of complex **2** in C_6D_6

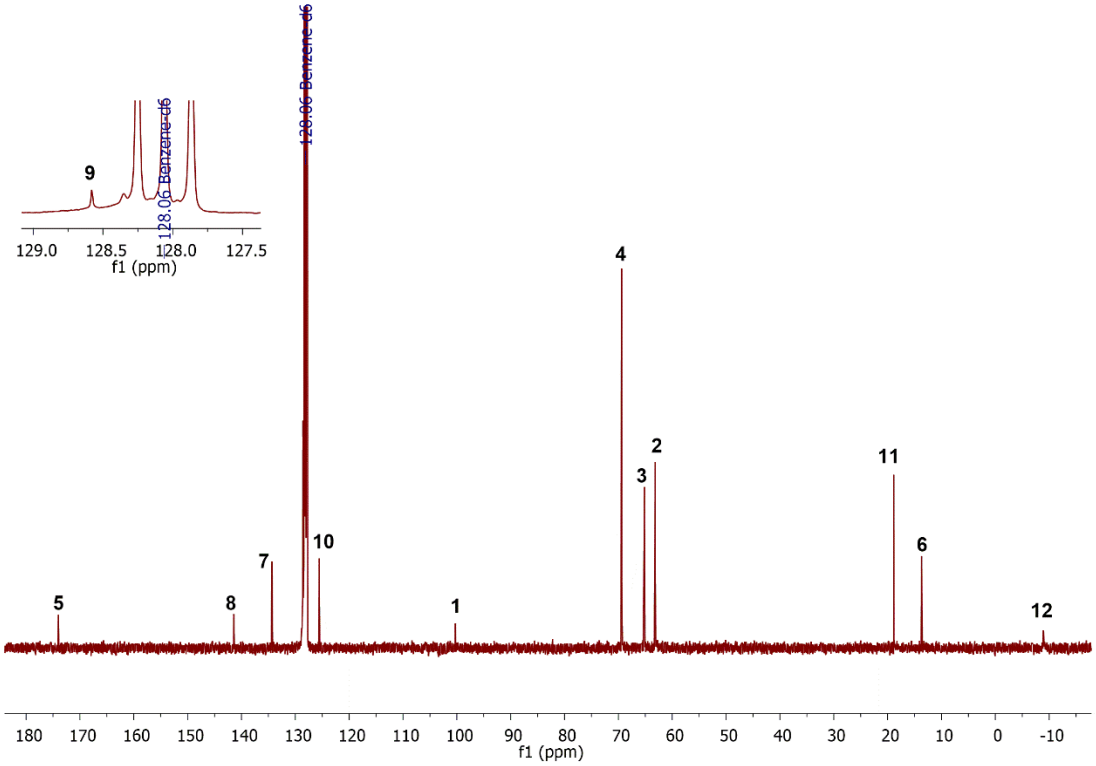

Figure S13. CVs at different scans rates of complex **2** (10^{-3} M) recorded in CH_2Cl_2 containing 0.2 M of *n*-Bu_4NPF_6.

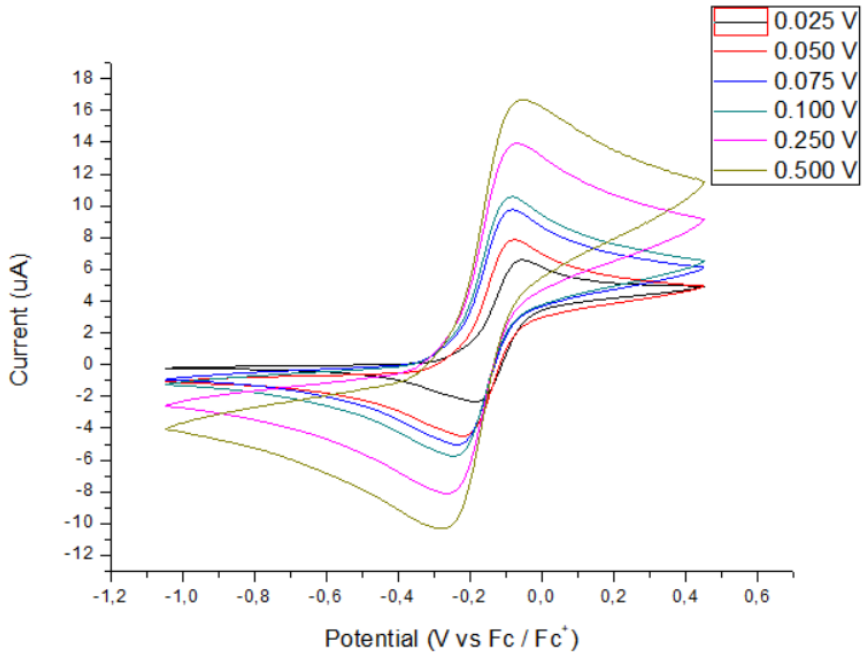

Aluminum complex 3, [(L$_1$)$_2$AlMe]. (Yield: 91%, 96 mg). **^{1}H, ^{13}C-HMBC** (400 MHz / 100 MHz, C_6D_6, 298 K): $\delta(^1H)$ / $\delta(^{13}C)$ = 7.19–7.11 / 139.19, 123.51, 28.50 (H_{9b} / $C_{7,9a,11b}$), 7.19–7.11 / 145.49, 144.81 (H_{10} / $C_{8a,b}$), 7.00 / 139.19, 123.82, 28.70 (H_{9a} / $C_{7,9b,11a}$), 3.73 / 101.42, 64.16, 63.15 (H_{2b} / $C_{1,2a,3a}$), 3.66 / 101.42, 64.16, 63.15 (H_{3b} / $C_{1,2a,3a}$), 3.66 / 101.42, 64.42, 59.42 (H_{3a} / $C_{1,3b,2b}$), 3.63–3.58 / 101.42, 64.42, 59.42 (H_{2a} / $C_{1,3b,2b}$), 3.63–3.58 / 139.19, 144.81, 123.82, 24.82, 24.34 (H_{11b} / $C_{7,8b,9b,12b,13b}$), 3.33–3.23 / 139.19, 145.49, 123.51, 25.18, 23.17 (H_{11a} / $C_{7,8a,9a,12a,13a}$), 1.86 / 172.61 (H_6 / C_5), 1.53 / 144.81, 28.50, 24.34 (H_{12b} / $C_{8b,11b,13b}$), 1.29 / 144.81, 28.50, 24.82 (H_{13b} / $C_{8b,11b,12b}$), 1.13 / 145.49, 28.70, 23.17 (H_{12a} / $C_{8a,11a,13a}$), 1.01 / 145.49, 28.70, 25.18 (H_{13a} / $C_{8a,11a,12a}$). **^{1}H, ^{13}C-HSQC** (400 MHz / 100 MHz, C_6D_6, 298 K): $\delta(^1H)$ / $\delta(^{13}C)$ = 7.19–7.11 / 123.82 (H_{9b} / C_{9b}), 7.19–7.11 / 126.31 (H_{10} / C_{10}), 7.00 / 123.51 (H_{9a} / C_{9a}), 4.11 / 69.13 (H_4 / C_4), 3.73 / 59.42 (H_{2b} / C_{2b}), 3.66 / 64.42 (H_{3b} / C_{3b}), 3.66 / 63.15 (H_{3a} / C_{3a}), 3.63 – 3.58 / 64.16 (H_{2a} / C_{2a}), 3.63–3.58 / 28.50 (H_{11b} / C_{11b}), 3.33–3.23 / 28.70 (H_{11a} / C_{11a}), 1.86 / 15.63 (H_6 / C_6), 1.53 / 24.82 (H_{12b} / C_{12b}), 1.29 / 24.34 (H_{13b} / C_{13b}), 1.13 / 25.18 (H_{12a} / C_{12a}), 1.01 / 23.17 (H_{13a} / C_{13a}), 0.23 / –9.42 (H_{14} / C_{14}). **^{1}H, ^{1}H-COSY** (400 MHz / 400 MHz, C_6D_6, 298 K): $\delta(^1H)$ / $\delta(^1H)$ = 7.19–7.11 / 7.19–7.11, 7.00 (H_{10}/ $H_{9b,a}$), 3.73 / 3.66 (H_{2b} / H_{3b}), 3.66 / 3.66 (H_{3b} / H_{3a}), 3.66 / 3.63–3.58 (H_{3a} / H_{2a}), 3.63–3.58 / 1.53, 1.29 (H_{11b} / $H_{12b,13b}$), 3.33–3.23 / 1.13, 1.01 (H_{11a} / $H_{12a,13a}$).

Figure S14. ^{1}H NMR spectrum of complex **3** in C_6D_6

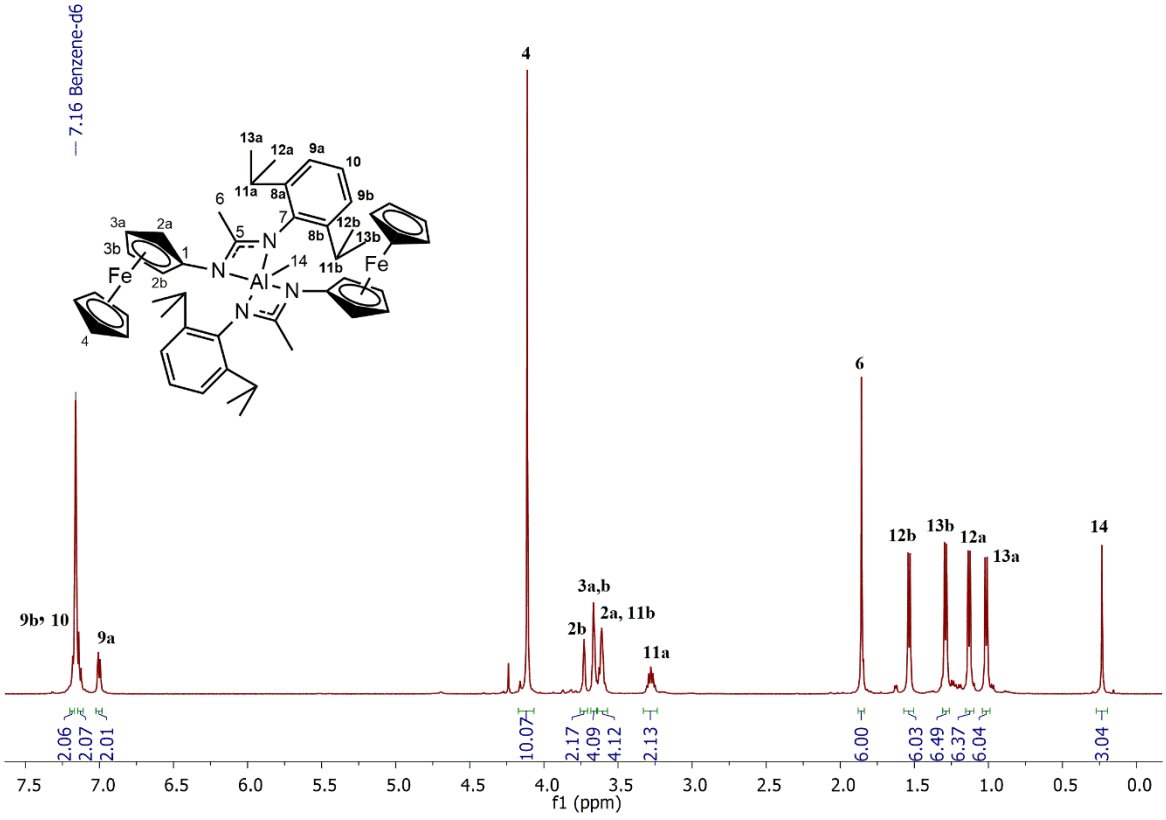

Figure S15. $^{13}C\{^{1}H\}$ NMR spectrum of complex **3** in C_6D_6

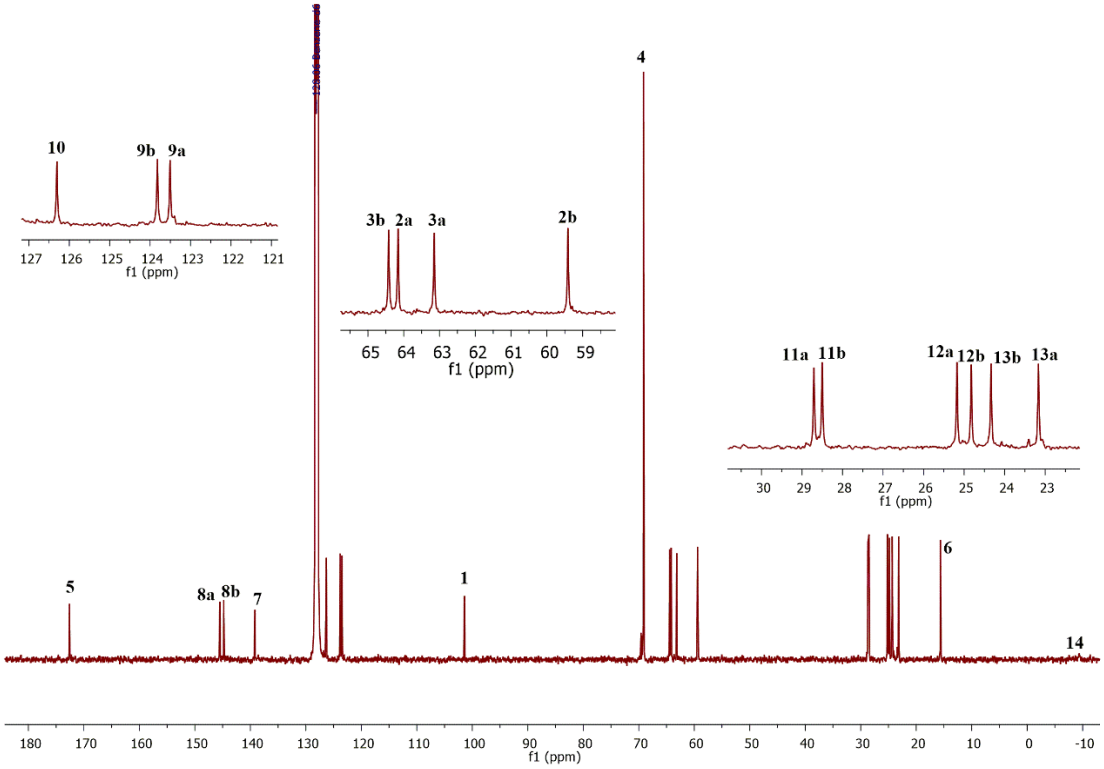

Figure S16. CVs at different scans rates of complex **3** (10^{-3} M) recorded in CH_2Cl_2 containing 0.2 M of *n*-Bu_4NPF_6.

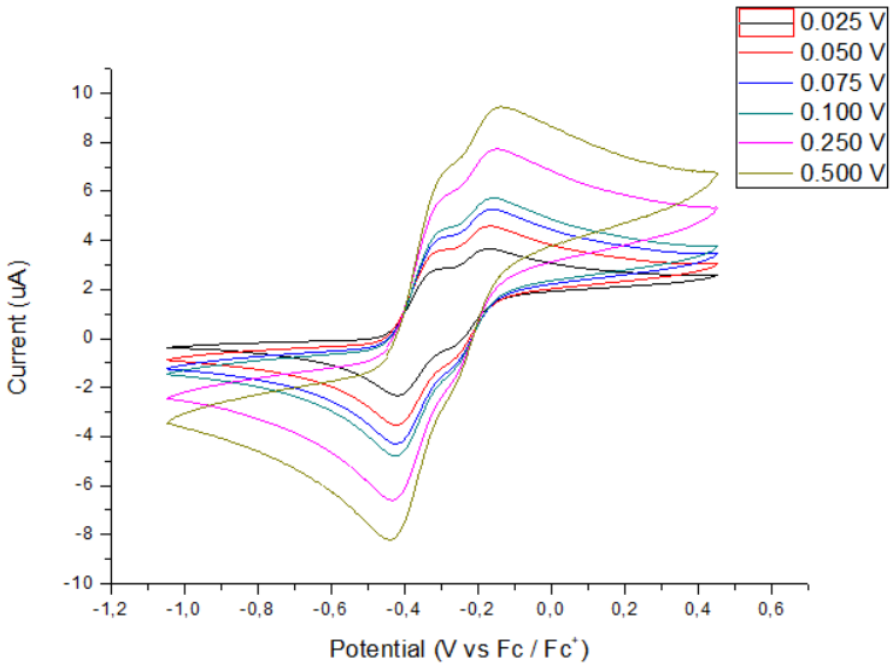

Figure S17. X ray crystal structure of complex **3**. Thermal ellipsoids are shown with 15% probability. Hydrogen atoms were omitted for clarity. Only one molecule (molecule "A") of two found in the asymmetric unit is shown

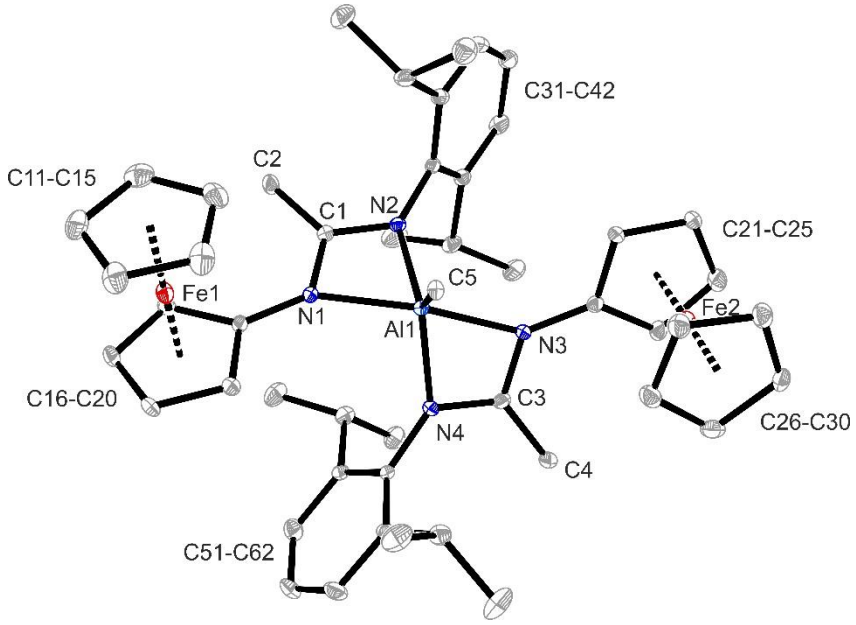

Aluminum complex 4, [(L2)2AlMe]. (Yield: 96%, 204 mg). **^{1}H, ^{13}C-HMBC** (400 MHz / 100 MHz, C_6D_6, 298 K): δ(^{1}H) / δ(^{13}C) = 7.09 / 142.75, 134.81, 128.35, 19.21 (H_{9a} / $C_{7,8a,9b,11a}$), 7.01 / 135.21, 134.81 (H_{10} / $C_{8b,a}$), 7.01 / 142.75, 135.21, 128.55, 19.48 (H_{9b} / $C_{7,8b,9a,11b}$), 3.70 / 101.37, 62.40 (H_{3a} / $C_{1,2b}$), 3.64 / 101.37, 62.40, 61.55 (H_{2a} / $C_{1,2b,3b}$), 3.60 / 101.37, 64.55, 64.51 (H_{2b} / $C_{1,3a,2a}$), 3.55 / 101.37, 64.55, 62.40 (H_{3b} / $C_{1,3a,2b}$), 2.35 / 142.75, 134.81, 128.55 (H_{11b} / $C_{7,8a,9a}$), 2.21 / 142.75, 135.21, 128.35 (H_{11a} / $C_{7,8b,9b}$), 1.73 / 172.45 (H_6 / C_5). **^{1}H, ^{13}C-HSQC** (400 MHz / 100 MHz, C_6D_6, 298 K): δ(^{1}H) / δ(^{13}C) = 7.09 / 128.55 (H_{9a} / C_{9a}), 7.01 / 125.37 (H_{10} / C_{10}), 7.01 / 128.35 (H_{9b} / C_{9b}), 4.03 / 69.20 (H_4 / C_4), 3.70 / 64.55 (H_{3a} / C_{3a}), 3.64 / 64.51 (H_{2a} / C_{2a}), 3.60 / 62.40 (H_{2b} / C_{2b}), 3.55 / 61.55 (H_{3b} / C_{3b}), 2.35 / 19.21 (H_{11a} / C_{11a}), 2.21 / 19.48 (H_{11b} / C_{11b}), 1.73 / 14.09 (H_6 / C_6), 0.07 / –8.49 (H_{12} / C_{12}). **^{1}H, ^{1}H-COSY** (400 MHz / 400 MHz, C_6D_6, 298 K): δ(^{1}H) / δ(^{1}H) = 7.09 / 7.01 (H_{9a}/ H_{10}), 7.01 / 7.01 (H_{10}/ H_{9b}), 3.70 / 3.64, 3.55 (H_{3a} / $H_{2a,3b}$), 3.60 / 3.55 (H_{2b} / H_{3b}).

Figure S18. ^{1}H NMR spectrum of complex **4** in C_6D_6

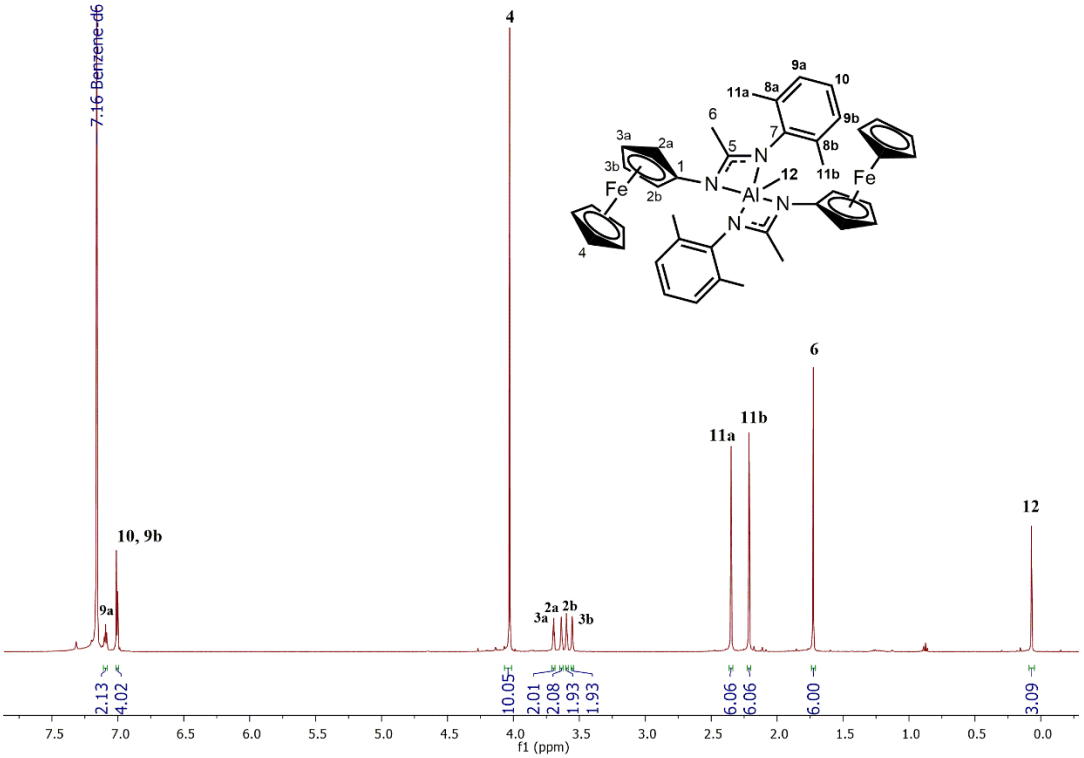

Figure S19. $^{13}C\{^{1}H\}$ NMR spectrum of complex **4** in C_6D_6

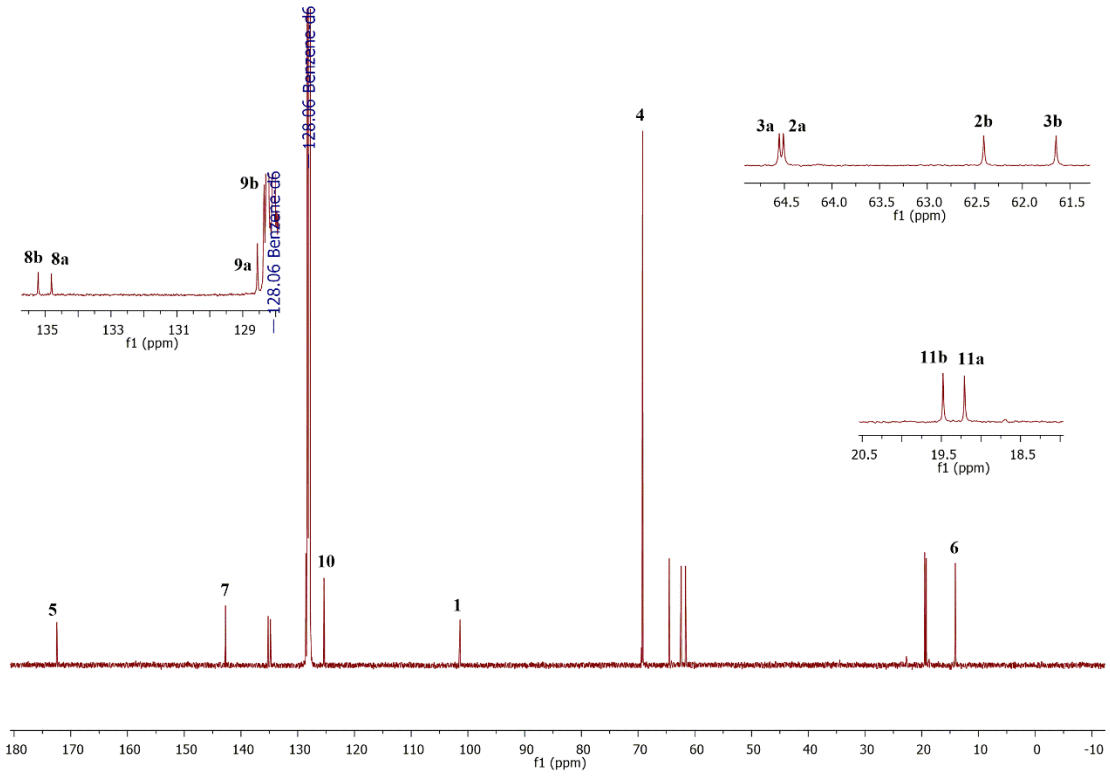

Figure S20. CVs at different scans rates of complex **4** (10^{-3} M) recorded in CH_2Cl_2 containing 0.2 M of *n*-Bu_4NPF_6.

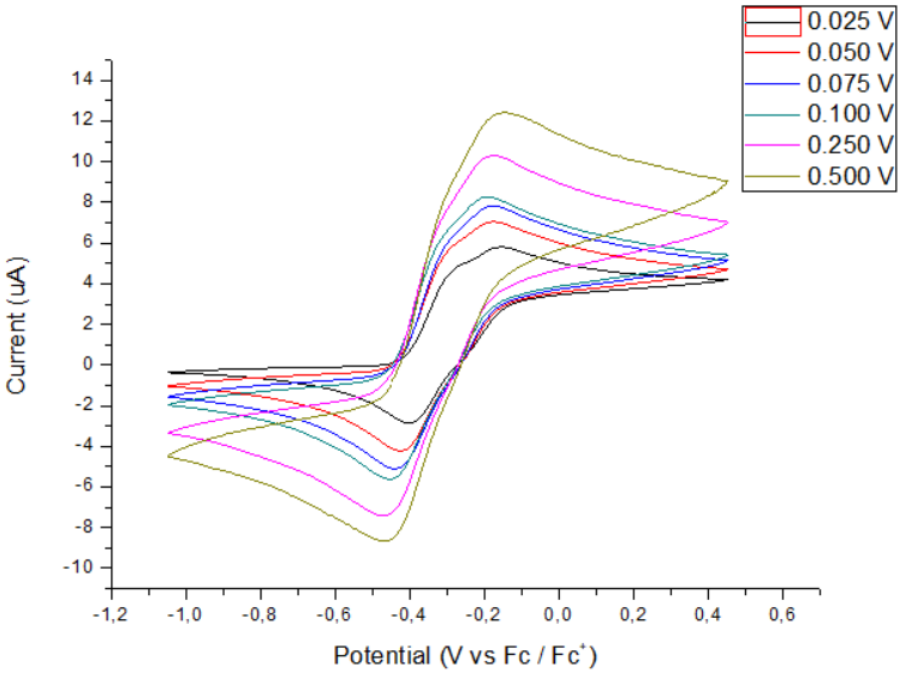

Figure S21. X ray crystal structure of complex **4**. Thermal ellipsoids are shown with 30% probability. Hydrogens atoms were omitted for clarity

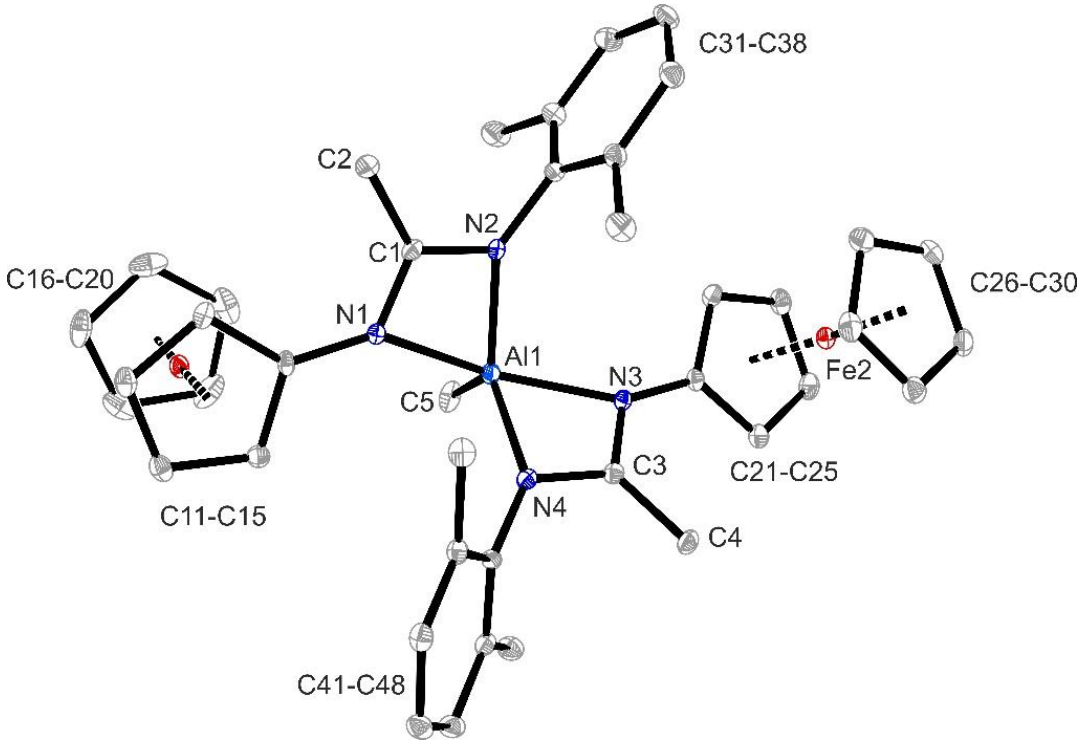

Table S1. Crystallographic data and structure refinement of complex **1**

	1
Empirical formula	$C_{26}H_{35}AlFeN_2$
Formula weight	458.39 g/mol
Temperature (K)	173(2)
Wavelength (Å)	0.71073
Crystal system	orthorhombic
Space group	Pbca
a(Å)	14.8404(2)
b(Å)	10.6928(1)
c(Å)	31.4241(5)
α(º)	90
β(º)	90
γ(º)	90
Volume($Å^3$)	4986.5(1)
Z	8
Density (calculated) (g/cm^3)	1.221
Absorption coefficient (mm^{-1})	0.654
F(000)	1952
Crystal size (mm^3)	0.20 x 0.10 x 0.02
Index ranges	$-17 \leq h \leq 17$ $-12 \leq k \leq 12$ $-37 \leq l \leq 37$
Reflections collected	8201
Independent reflections	4374 [R(int) = 0.0364]
Data/restraints/parameters	4374 / 0 / 278
Goodness-of-fit on F^2	1.067
Final R indices [I>2σ(I)]	R1 = 0.0397, wR2 = 0.0876
R indices (all data)	R1 = 0.0510 wR2 = 0.0943
Largest diff. peak / hole, $e.Å^{-3}$	0.246 and -0.261

Table S2. Bond distances (Å) and angles (º) of complex **1**

1 (Bond distances, Å)	
Al1 – N2	1.936 (2)
Al1 – N1	1.941 (2)
Al1 – C4	1.950 (3)
Al1 – C3	1.956 (3)
C1 – N2	1.335 (3)
C1 – N1	1.332 (3)
C1 – C2	1.486 (3)
N2 – C31	1.408 (3)
N1 – C11	1.432 (3)
C11 – C12	1.396 (3)
C11 – C16	1.400 (3)
C16 – C20	1.525 (4)
Fe1 – C31	2.059 (2)
Fe1 – C36	2.036 (3)
1 (Bond angles, º)	
N2 – Al1 – N1	68.26 (8)
N2 – Al1 – C4	112.86 (12)
N1 – Al1 – C3	114.49 (12)
C4 – Al1 – C3	119.59 (15)
N2 – C1 – N1	109.3 (2)
N2 – C1 – C2	126.4 (2)
N1 – C1 – C2	124.2 (2)
C1 – N1 – C11	123.4 (2)
C1 – N1 – Al1	91.13 (14)
C31 – N2 – C1	127.1 (2)
C1 – N2 – Al1	91.23 (14)
C40 – Fe1 – C31	106.84 (10)
C40 – Fe1 – C38	67.98 (12)
Fe1 – C31 – N2	128.30 (16)

Table S3. Crystallographic data and structure refinement for complexes **3** and **4**

	3	**4**
Empirical formula	$C_{49}H_{61}AlFe_2N_4$	$C_{41}H_{45}AlFe_2N_4$
Formula weight	844.69 g/mol	732.49 g/mol
Temperature (K)	173(2)	100(2)
Wavelength (Å)	0.71073	1.54178
Crystal system	monoclinic	monoclinic
Space group	$P2_1/n$	$C2/c$
a(Å)	19.7132(4)	20.6079(2)
b(Å)	15.7957(3)	8.0992(7)
c(Å)	28.5412(7)	43.270(4)
α(º)	90	90
β(º)	90.080(1)	101.284(4)
γ(º)	90	90
Volume($Å^3$)	8887.3(3)	7082.5(11)
Z	8	8
Density (calculated) (g/cm^3)	1.263	1.374
Absorption coefficient (mm^{-1})	0.710	7.074
F(000)	3584	3072
Crystal size (mm^3)	0.21 x 0.18 x 0.15	0.1 x 0.18 x 0.22
Index ranges	$-24 \leq h \leq 24$ $-19 \leq k \leq 19$ $0 \leq l \leq 35$	$-24 \leq h \leq 23$ $-9 \leq k \leq 9$ $-51 \leq l \leq 51$
Reflections collected	18070	39924
Independent reflections	18073 [R(int) = 0.139]	6238 [R(int) = 0.0793]
Data/restraints/parameters	18070 / 0 / 1010	6238 / 0 / 440
Goodness-of-fit on F^2	1.023	1.113
Final R indices [I>2σ(I)]	R1 = 0.0663 wR2 = 0.1470	R1 = 0.0430 wR2 = 0.1067
R indices (all data)	R1 = 0.1017 wR2 = 0.1670	R1 = 0.0543 wR2 = 0.1104
Largest diff. peak / hole, $e.Å^{-3}$	0.510 and -0.453	0.338 and -0.446

Table S4. Bond distances (Å) and angles (º) for complexes **3** and **4**

3 (Bond distances, Å)		**4 (Bond distances, Å)**	
Al1 – N1	2.020 (4)	Al1 – N1	2.029 (2)
Al1 – N2	1.927 (4)	Al1 – N2	1.934 (2)
Al1 – N3	2.026 (4)	Al1 – N3	2.028 (2)
Al1 – N4	1.930 (4)	Al1 – N4	1.944 (2)
Al1 – C5	1.984 (5)	Al1 – C5	1.964 (3)
C1 – N1	1.332 (6)	C1 – N1	1.331 (3)
C1 – N2	1.330 (6)	C1 – N2	1.340 (3)
C1 – C2	1.491 (7)	C1 – C2	1.492 (4)
C3 – N3	1.331 (6)	C3 – N3	1.326 (4)
C3 – N4	1.332 (6)	C3 – N4	1.343 (4)
C3 – C4	1.499 (7)	C3 – C4	1.499 (4)
N1 – C11	1.396 (6)	N1 – C11	1.392 (3)
N3 – C21	1.402 (6)	N3 – C21	1.395 (3)
N4 – C51	1.424 (6)	N4 – C41	1.426 (3)
3 (Bond angles, º)		**4 (Bond angles, º)**	
N2 – Al1 – N1	66.52 (16)	N2 – Al1 – N1	66.50 (9)
N2 – Al1 – N4	125.24 (18)	N2 – Al1 – N4	123.09 (11)
N2 – Al1 – C5	118.0 (2)	N2 – Al1 – C5	119.75 (13)
N2 – C1 – N1	108.9 (4)	N2 – C1 – N1	109.0 (2)
N2 – Al1 – N3	100.30 (17)	N2 – Al1 – N3	99.12 (10)
N2 – C1 – C2	125.5 (4)	N2 – C1 – C2	124.0 (3)
N3 – Al1 – N4	66.45 (17)	N3 – Al1 – N4	66.84 (10)
N3 – Al1 – N1	150.38 (18)	N3 – Al1 – N1	151.63 (11)
N3 – C3 – N4	109.1 (4)	N3 – C3 – N4	110.2 (3)
C1 – N1 – C11	128.3 (4)	C1 – N1 – C11	127.2 (3)
C1 – N2 – C31	125.6 (4)	C1 – N2 – C31	122.0 (2)
C3 – N4 – C51	126.7 (4)	C3 – N4 – C41	122.6 (2)
C3 – N3 – C21	127.7 (4)	C3 – N3 – C21	126.0 (3)
Fe1 – C11 – N1	127.6 (4)	Fe1 – C11 – N1	126.84(19)

3. Structural Characterization for Cyclic Carbonates 6a–j.

Styrene carbonate (6a). (Conv: 100%; Yield: 97%, 270.7 mg); ^{1}H NMR, $CDCl_3$: δ/ppm = 7.43–7.36 (3H, m, ArH), 7.35–7.30 (2H, m, ArH), 5.65 (1H, t *J* = 8.0 Hz, PhCHO), 4.77 (1H, t *J* = 8.4 Hz, OCH_2), 4.29 (1H, t *J* = 8.0 Hz, OCH_2); ^{13}C{^{1}H} NMR, $CDCl_3$: δ/ppm = 155.0, 135.9, 129.7, 129.2, 126.0, 78.1, 71.2.

Figure S22. ^{1}H NMR spectrum of styrene carbonate **6a** in $CDCl_3$

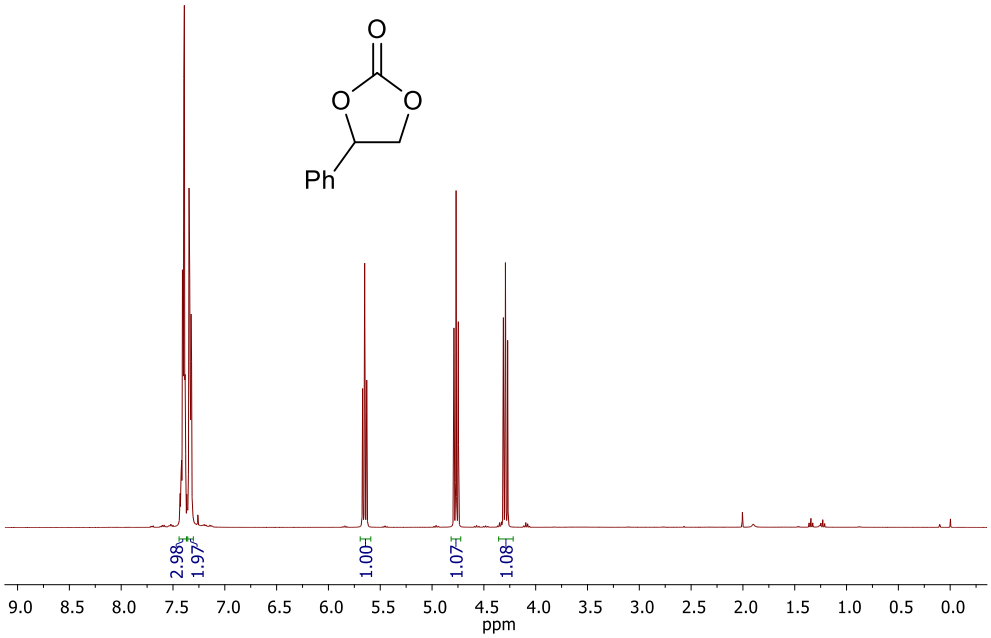

Figure S23. ^{13}C{^{1}H} NMR spectrum of styrene carbonate **6a** in $CDCl_3$

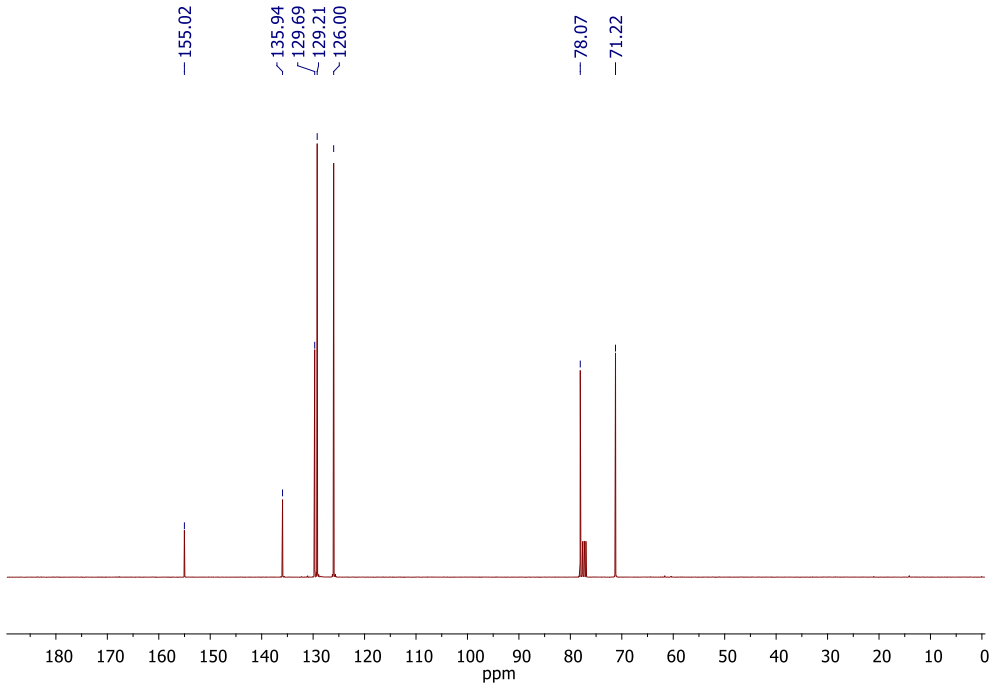

Propylene carbonate (6b). (Conv: n.d.; Yield: 85%, 147.5 mg); ^{1}H NMR, $CDCl_3$: δ/ppm = 4.85–4.76 (1H, m, OCH), 4.50 (1H, dd *J* = 8.3, 7.8 Hz, OCH_2), 3.98 (1H, dd *J* = 8.4, 7.2 Hz, OCH_2), 1.44 (3H, d *J* = 6.3 Hz, CH_3); $^{13}C\{^{1}H\}$ NMR, $CDCl_3$: δ/ppm = 155.1, 73.6, 70.7, 19.4.

Figure S24. ^{1}H NMR spectrum of propylene carbonate **6b** in $CDCl_3$

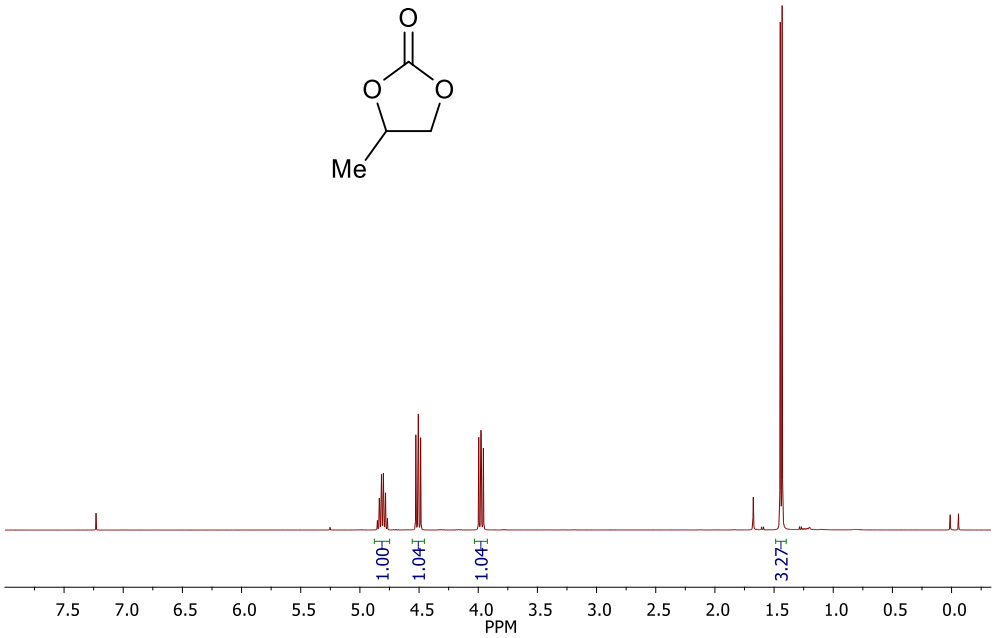

Figure S25. $^{13}C\{^{1}H\}$ NMR spectrum of propylene carbonate **6b** in $CDCl_3$

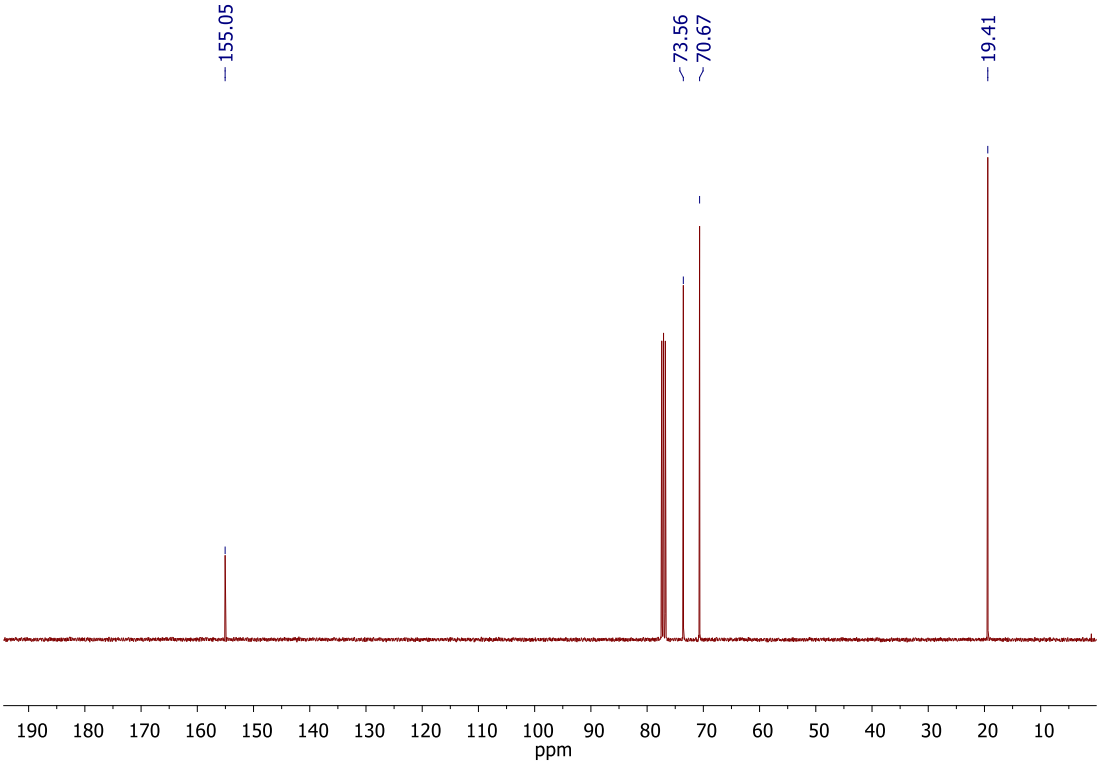

1,2-Butylene carbonate (6c). (Conv: 99%; Yield: 82%, 167.8 mg). ^{1}H NMR, $CDCl_3$: δ/ppm = 4.65–4.59 (1H, m, OCH), 4.49 (1H, t *J* = 8.1 Hz, OCH_2), 4.04 (1H, dd *J* = 8.3, 7.2 Hz, OCH_2), 1.84–1.65 (2H, m, CH_2) 0.99 (3H, t *J* = 7.5 Hz, CH_3); $^{13}C\{^{1}H\}$ NMR, $CDCl_3$: δ/ppm = 155.1, 78.0, 69.0, 27.0, 8.5.

Figure S26. ^{1}H NMR spectrum of 1,2-butylene carbonate **6c** in $CDCl_3$

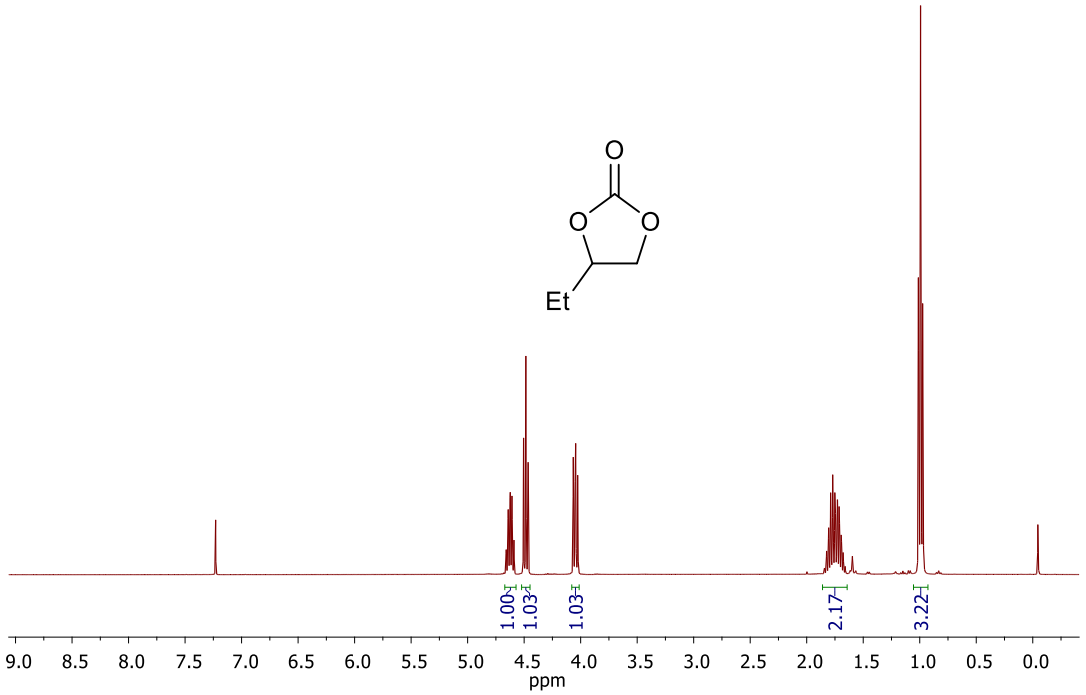

Figure S27. $^{13}C\{^{1}\}$ NMR spectrum of 1,2-butylene carbonate **6c** in $CDCl_3$

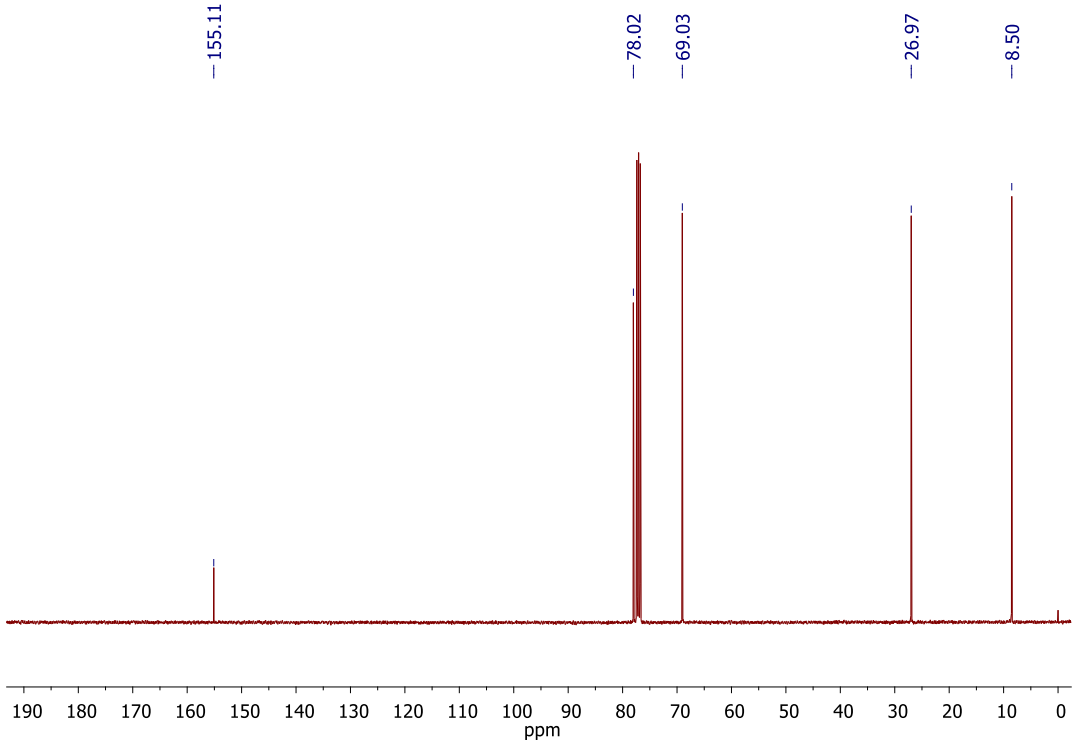

1,2-Hexylene carbonate (6d). (Conv: 99%; Yield: 70%, 171.4 mg); ^{1}H NMR, $CDCl_3$: δ/ppm = 4.71–4.62 (1H, m OCH), 4.49 (1H, t *J* = 8.1 Hz, OCH_2), 4.03 (1H, dd *J* = 8.3, 7.2 Hz, OCH_2), 1.85–1.72 (1H, m, CH_2), 1.70–1.61 (1H, m, CH_2), 1.46–1.28 (4H, m, 2 x CH_2), 0.89 (3H, t *J* = 6.8 Hz, CH_3); ^{13}C{^{1}H} NMR, $CDCl_3$: δ/ppm = 155.1, 77.1, 69.4, 33.6, 26.5, 22.3, 13.8.

Figure S28. ^{1}H NMR spectrum of 1,2-hexylene carbonate **6d** in $CDCl_3$

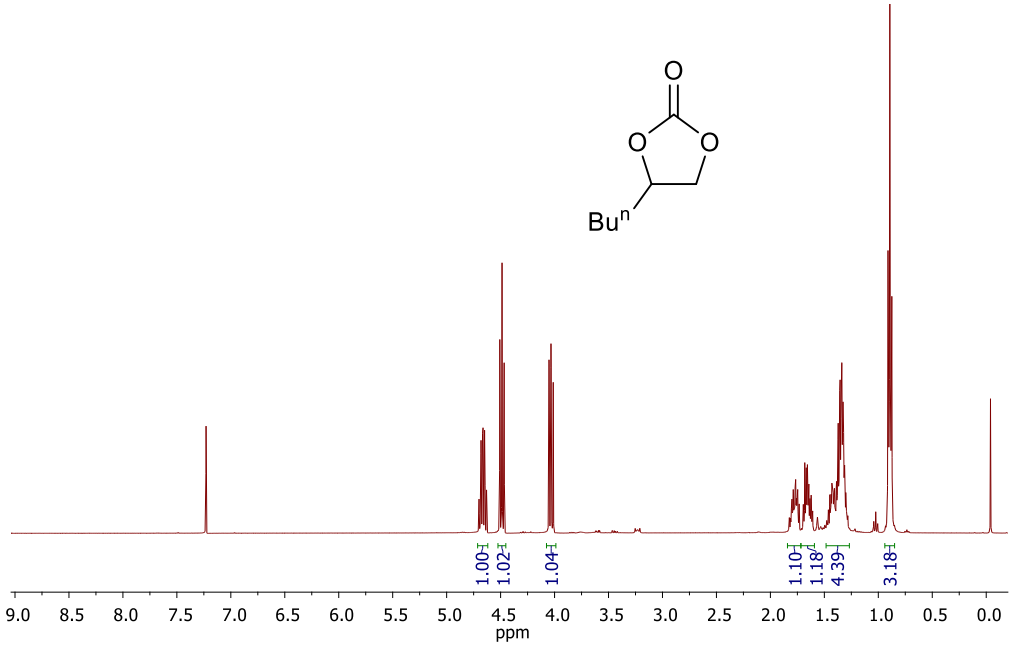

Figure S29. ^{13}C{^{1}H} NMR spectrum of 1,2-hexylene carbonate **6d** in $CDCl_3$

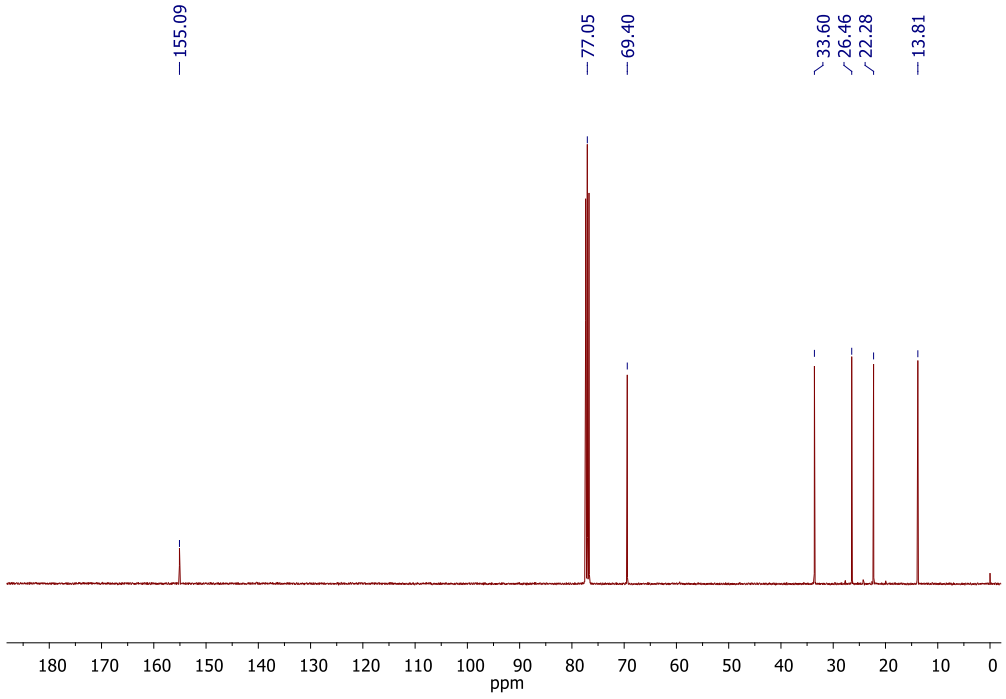

Glycerol carbonate (6e). (Conv: 99%; Yield: 87%, 174.7 mg); ^{1}H NMR, DMSO-D$_6$: δ/ppm = 5.25 (1H, t *J* = 5.6 Hz, OH), 4.84–4.76 (1H, m, OCH), 4.50 (1H, t *J* = 8.3 Hz, CH_2O), 4.29 (1H, dd *J* = 10.2, 5.1 Hz, CH_2O), 3.70–3.64 (1H, m, CH_2OH), 3.54–3.48 (1H, m, CH_2OH); ^{13}C{^{1}H} NMR, DMSO-D$_6$: δ/ppm = 155.6, 77.5, 66.3, 61.1.

Figure S30. ^{1}H NMR spectrum of glycerol carbonate **6e** in DMSO-D$_6$

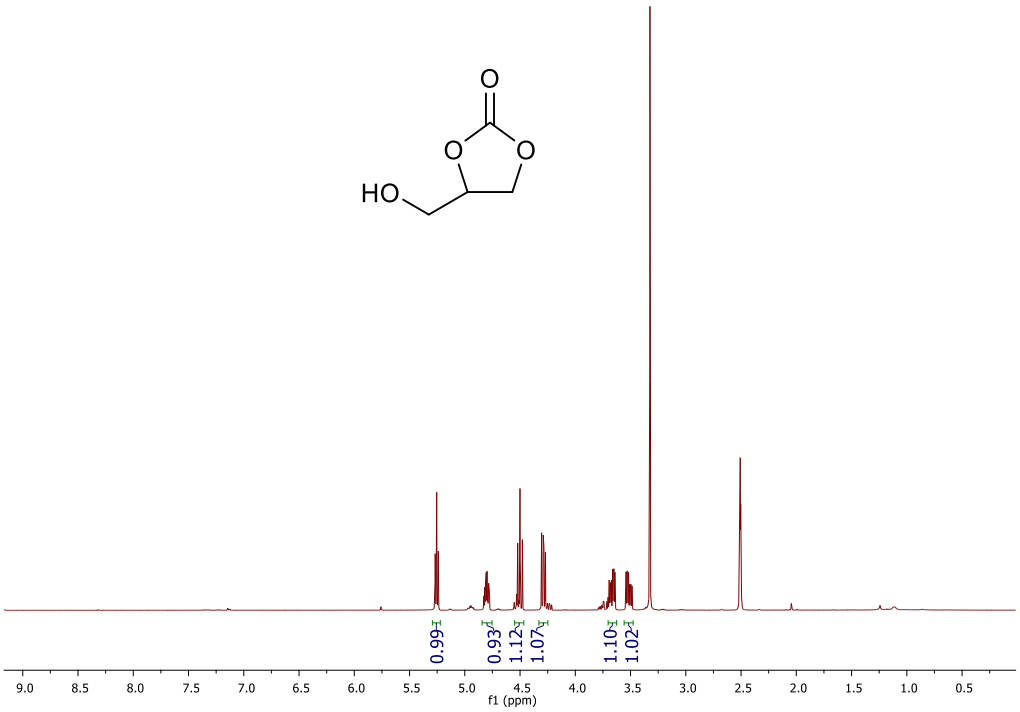

Figure S31. ^{13}C{^{1}H} NMR spectrum of glycerol carbonate **6e** in DMSO-D$_6$

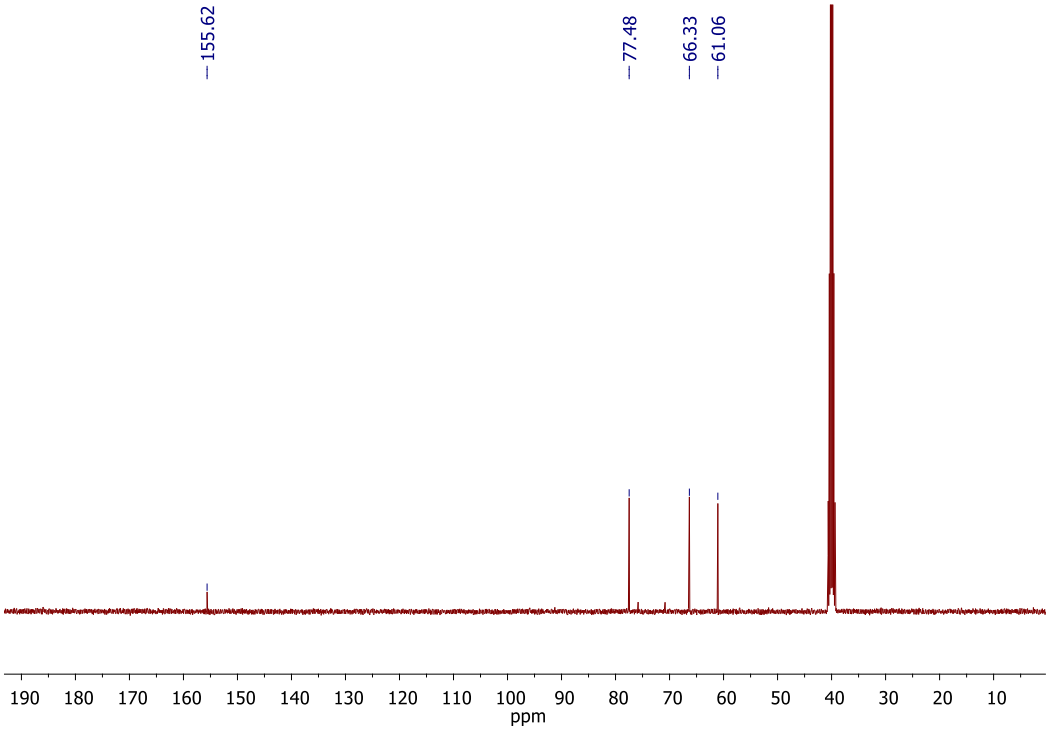

3-Phenoxyproplylene carbonate (6f). (Conv: 81%; Yield: 71%, 234.3 mg); ^{1}H NMR, $CDCl_3$: δ/ppm = 7.37–7.27 (2H, m, 2 x ArH), 7.03 (1H, t *J* = 7.5 Hz, ArH), 6.96–6.89 (2H, m, 2 x ArH), 5.08–4.98 (1H, m, OCH), 4.62 (1H, t *J* = 8.4 Hz, OCH_2), 4.54 (1H, dd *J* = 8.5, 5.9 Hz, OCH_2), 4.24 (1H, dd *J* = 10.6, 4.3 Hz, CH_2OPh), 4.16 (1H, dd *J* = 10.6, 3.6 Hz, CH_2OPh); $^{13}C\{^{1}H\}$NMR, $CDCl_3$: δ/ppm = 157.8, 154.6, 129.7, 122.0, 114.6, 74.1, 66.9, 66.3.

Figure S32. ^{1}H NMR spectrum of 3-phenoxyproplylene carbonate **6f** in $CDCl_3$

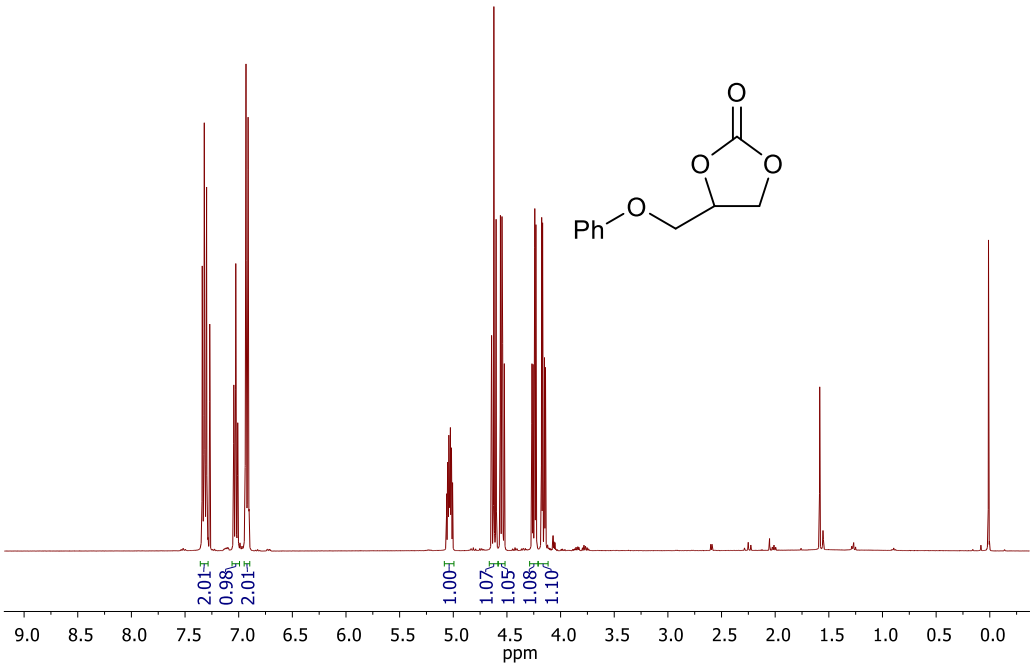

Figure S33. $^{13}C\{^{1}H\}$ NMR spectrum of 3-phenoxyproplylene carbonate **6f** in $CDCl_3$

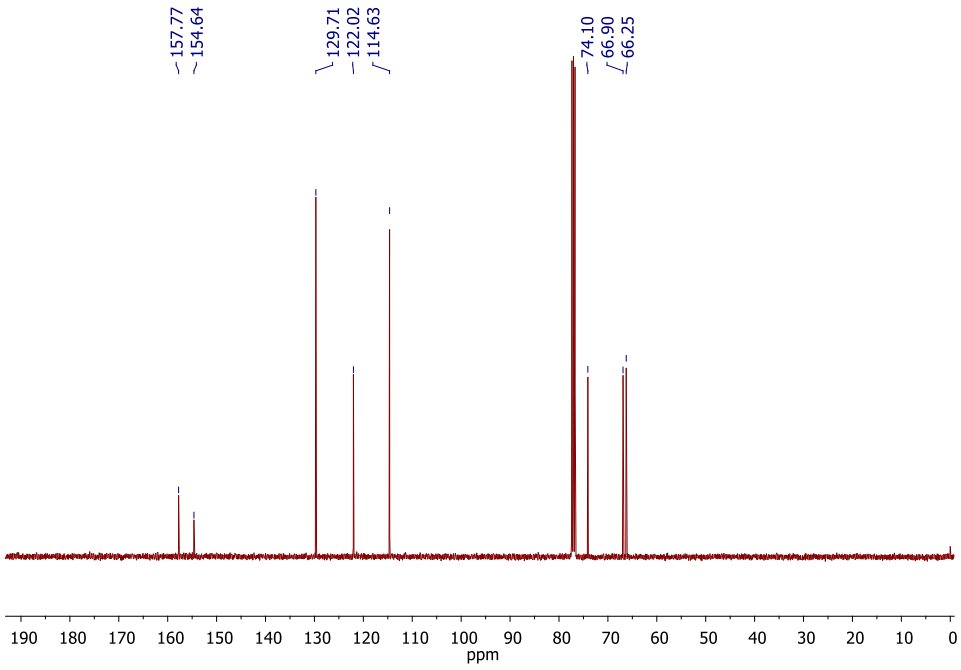

3-Chloropropylene carbonate (6g). (Conv: 99%; Yield: 98%, 227.4 mg); ^{1}H NMR, $CDCl_3$: δ/ppm = 4.97–4.91 (1H, m, OCH), 4.54 (1H, t *J* = 8.6 Hz, CH_2O), 4.35 (1H, dd *J* = 8.9, 5.7 Hz, CH_2O), 3.76 (1H, dd *J* = 12.2, 5.1 Hz, CH_2Cl), 3.67 (1H, dd *J* = 12.5, 4.0 Hz, CH_2Cl); $^{13}C\{^{1}H\}$ NMR, $CDCl_3$: δ/ppm = 154.4, 74.5, 67.0, 44.0.

Figure S34. ^{1}H NMR spectrum of 3-chloropropylene carbonate **6g** in $CDCl_3$

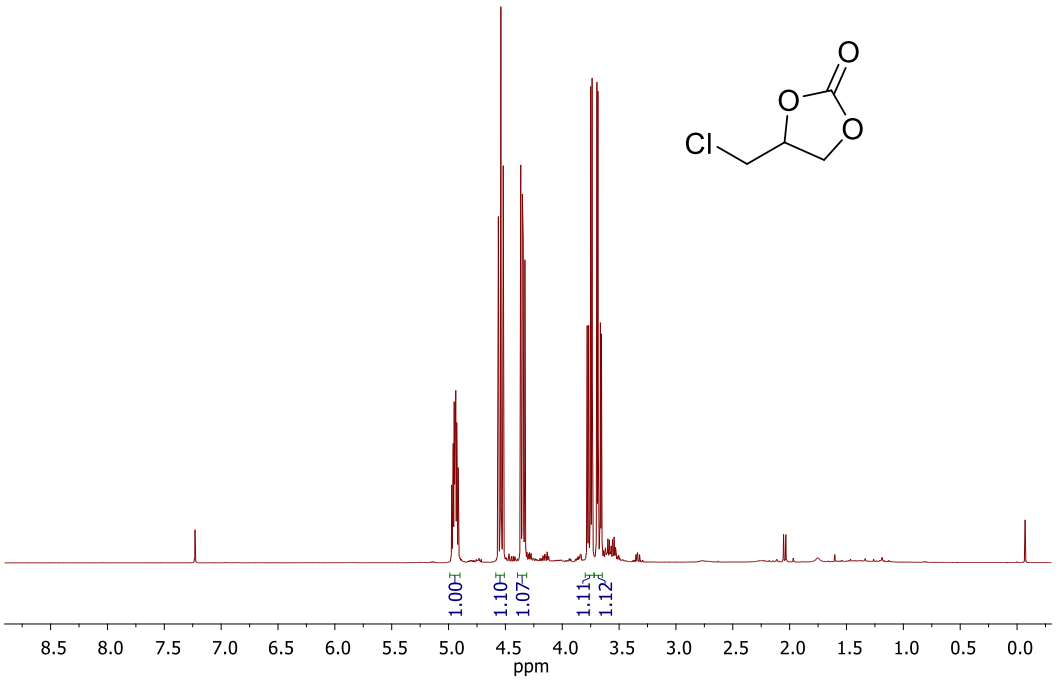

Figure S35. $^{13}C\{^{1}H\}$ NMR spectrum of 3-chloropropylene carbonate **6g** in $CDCl_3$

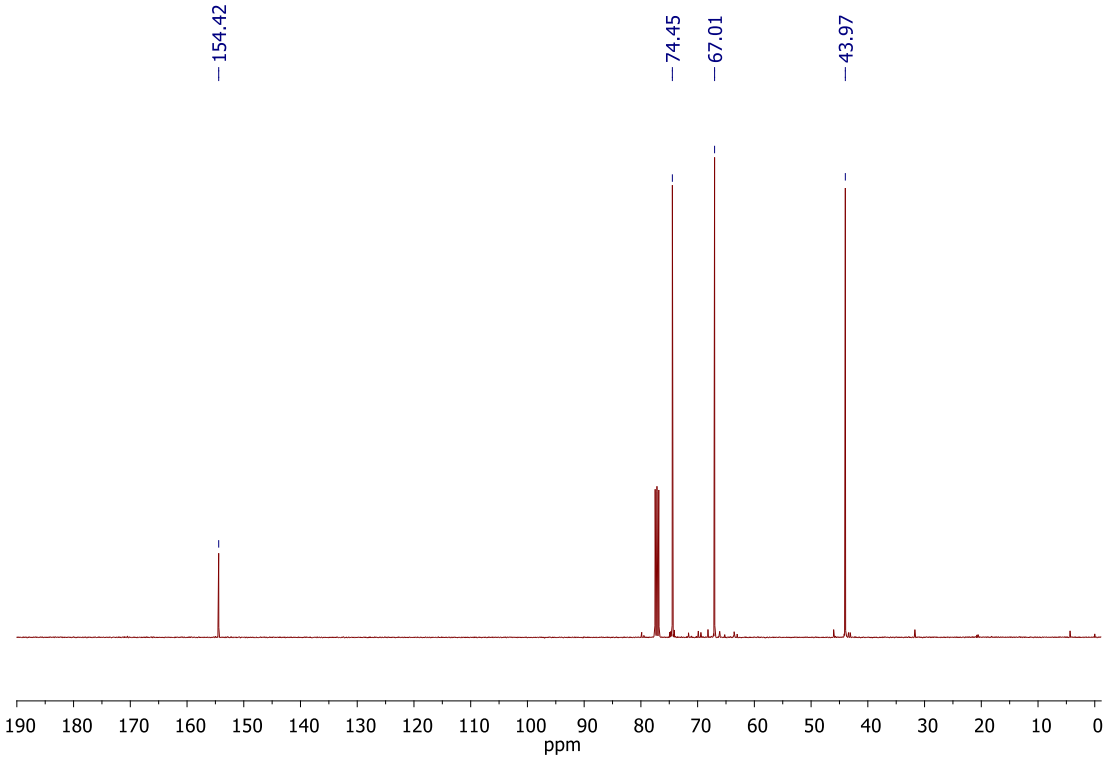

4-Bromostyrene carbonate (6h). (Conv: 99%; Yield: 80%, 330.6 mg); ^{1}H NMR, $CDCl_3$: δ/ppm = 7.42–7.38 (2H, m, ArH), 7.31–7.28 (2H, m, ArH), 5.61 (1H, t *J* = 8.0 Hz, OCH), 4.77 (1H, t *J* = 8.5 Hz, OCH_2), 4.27 (1H, dd *J* = 8.7, 7.8 Hz, OCH_2); ^{13}C{^{1}H} NMR, $CDCl_3$: δ/ppm = 154.4, 134.8, 132.5, 127.4, 127.2, 77.2, 70.9.

Figure S36. ^{1}H NMR spectrum of 4-bromostyrene carbonate **6h** in $CDCl_3$

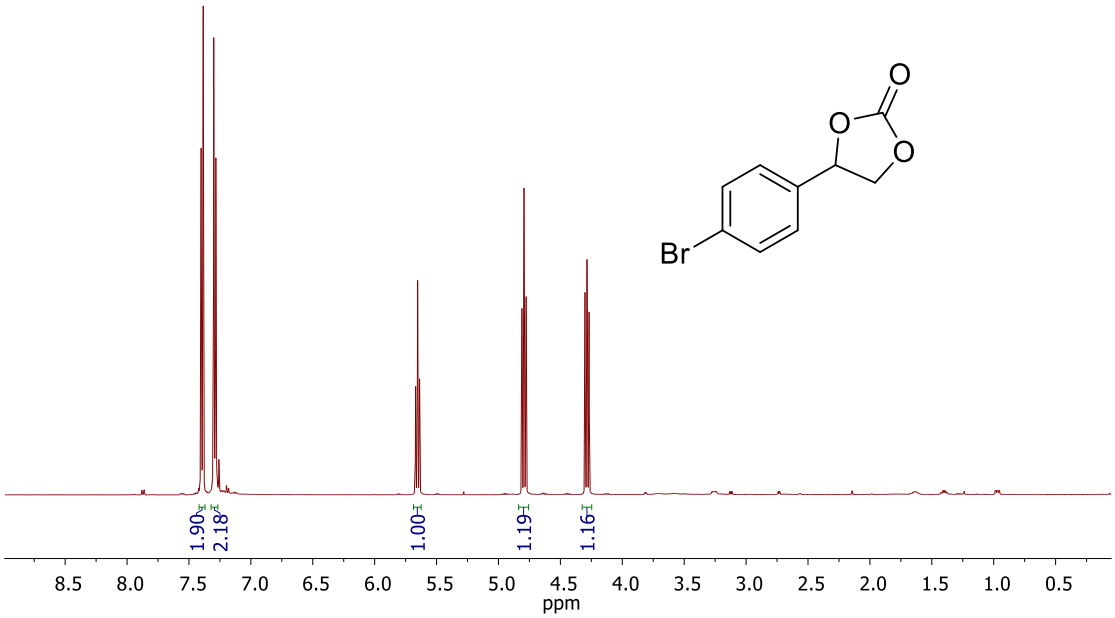

Figure S37. ^{13}C{^{1}H} NMR spectrum of 4-bromostyrene carbonate **6h** in $CDCl_3$

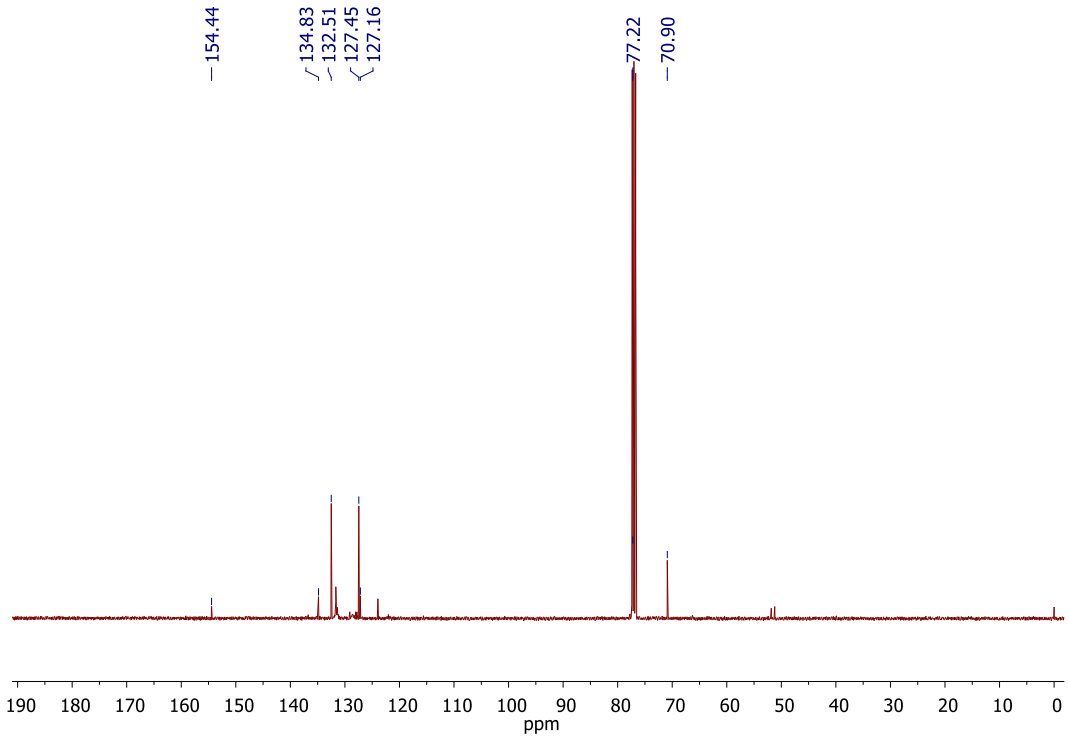

4-((2,2,3,3-Tetrafluoropropoxy)methyl)-1,3-dioxolan-2-one (6i). (Conv: 99%; Yield: 97%, 384.4 mg). ^{1}H NMR, $CDCl_3$: δ/ppm = 5.83 (1H, tt *J* = 52.8, 4.8 Hz, $CHCF_2$), 4.75–4.82 (1H, m, OCH), 4.46 (1H, t *J* = 7.6 Hz, OCH_2), 4.31 (1H, dd *J* = 7.6, 6.0 Hz, OCH_2), 3.85 (2H, dt *J* = 12.8, 2.0 Hz, OCH_2CF_2), 3.78 (1H, dd *J* = 11.2, 3,2 Hz, O*CH*$_2$CH), 3.69 (1H, dd *J* = 11.2, 4.0 Hz, O*CH*$_2$CH); ^{13}C{^{1}H} NMR, $CDCl_3$: δ/ppm = 153.9 (C=O), 113.9 (tt *J* = 994.0, 107.6 Hz, CH*CF*$_2$), 108.2 (tt *J* = 991.6, 138.8 Hz, CF_2), 73.8 (CH), 70,4 (CH_2), 67.4 (t *J* = 112.4 Hz, CF_2*CH*$_2$), 64.9 (CH_2); ^{19}F NMR, $CDCl_3$: δ/ppm = (−139.2)–(−139.1) (m, 2F), (−124.9)–(−124.8) (m, 2F).

Figure S38. ^{1}H NMR spectrum of 4-((2,2,3,3-Tetrafluoropropoxy)methyl)-1,3-dioxolan-2-one **6i** in $CDCl_3$

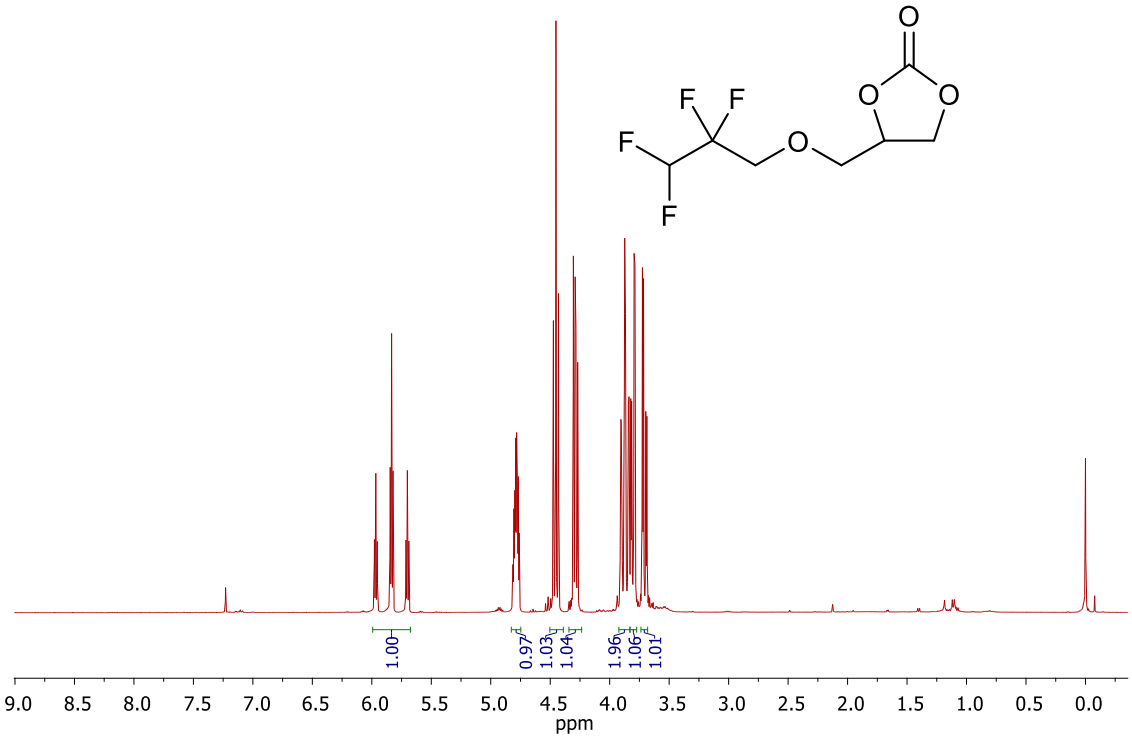

Figure S39. $^{13}C\{^{1}H\}$ NMR spectrum of 4-((2,2,3,3-Tetrafluoropropoxy)methyl)-1,3-dioxolan-2-one **6i** in $CDCl_3$

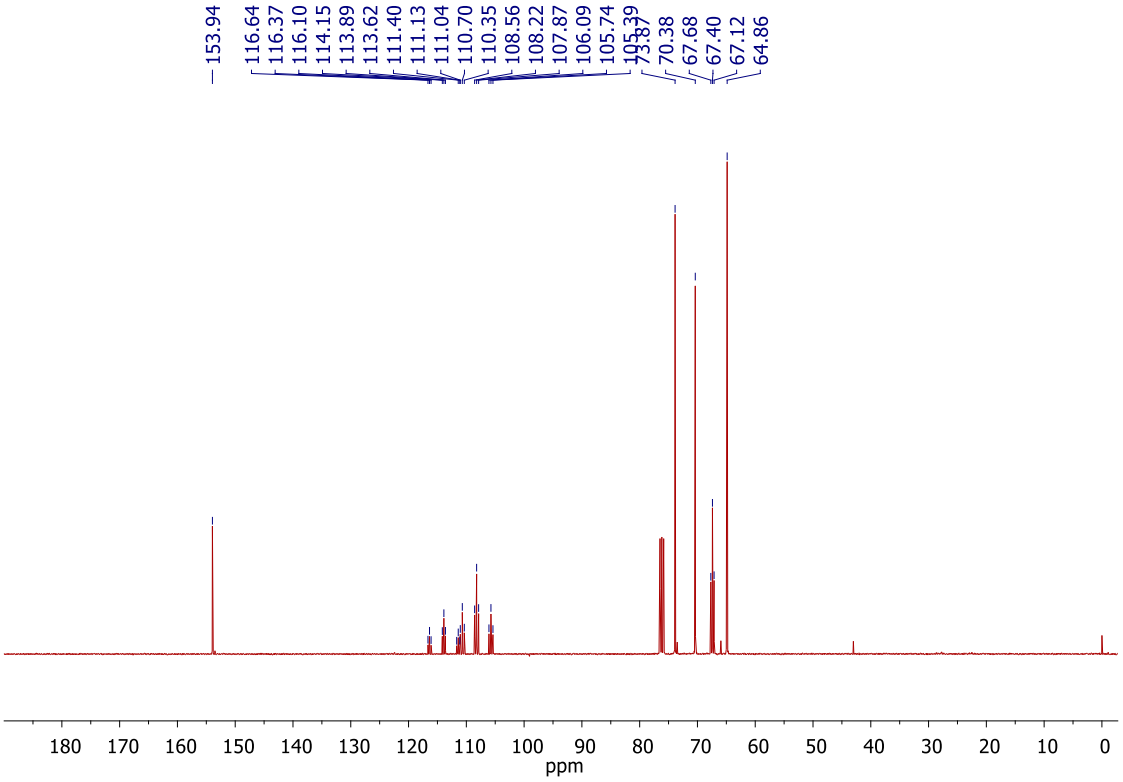

Figure S40. ^{19}F NMR spectrum of 4-((2,2,3,3-Tetrafluoropropoxy)methyl)-1,3-dioxolan-2-one **6i** in $CDCl_3$

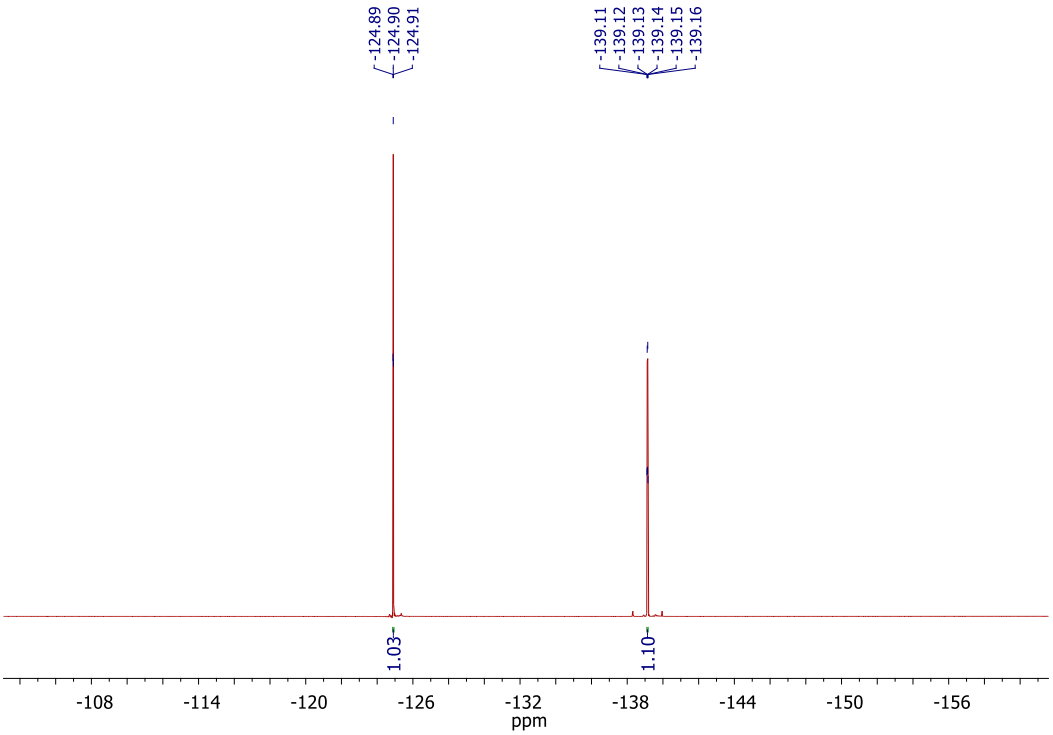

4-(((2,2,3,3,4,4,5,5-Octafluoropentyl)oxy)methyl)-1,3-dioxolan- 2-one (6j). (Conv: 99%; Yield: 94%, 535.6 mg). ^{1}H NMR, $CDCl_3$: δ/ppm = 6.03 (1H, tt *J* = 52.0, 5.6 Hz, CHF_2), 4.84–4.78 (1H, m, OCH), 4.45 (1H, t *J* = 8.8 Hz, OCH_2), 4.31 (1H, dd *J* = 8.4, 6.0 Hz, OCH_2), 4.11–3.91 (2H, m, OCH_2CF_2), 3.81 (1H, dd *J* = 11.2, 3,2 Hz, O*CH*$_2$CH), 3.77 (1H, dd *J* = 11.2, 3.6 Hz, O*CH*$_2$CH); ^{13}C{^{1}H} NMR, $CDCl_3$: δ/ppm = 154.1 (C=O), 117.1–104.1 (m, 3 x CF_2), 114.6 (tt *J* = 1020.4, 121.6 Hz, CH*CF*$_2$), 106.9 (tt *J* = 1009.2, 122.4 Hz, CF_2), 74.0 (CH), 70,8 (CH_2), 67.5 (t, *J* = 102.8 Hz, CF_2*CH*$_2$), 67.0 (CH_2); ^{19}F NMR $CDCl_3$: δ/ppm = (−137.9)–(−136.8) (m, 2F), (−130.6)–(−130.5) (m, 2F), (−125.8)–(−125.7) (m, 2F), (−120.3)– (−120.2) (m, 2F).

Figure S41. ^{1}H NMR spectrum of 4-(((2,2,3,3,4,4,5,5-Octafluoropentyl)oxy)methyl)-1,3-dioxolan-2-one **6j** in $CDCl_3$.

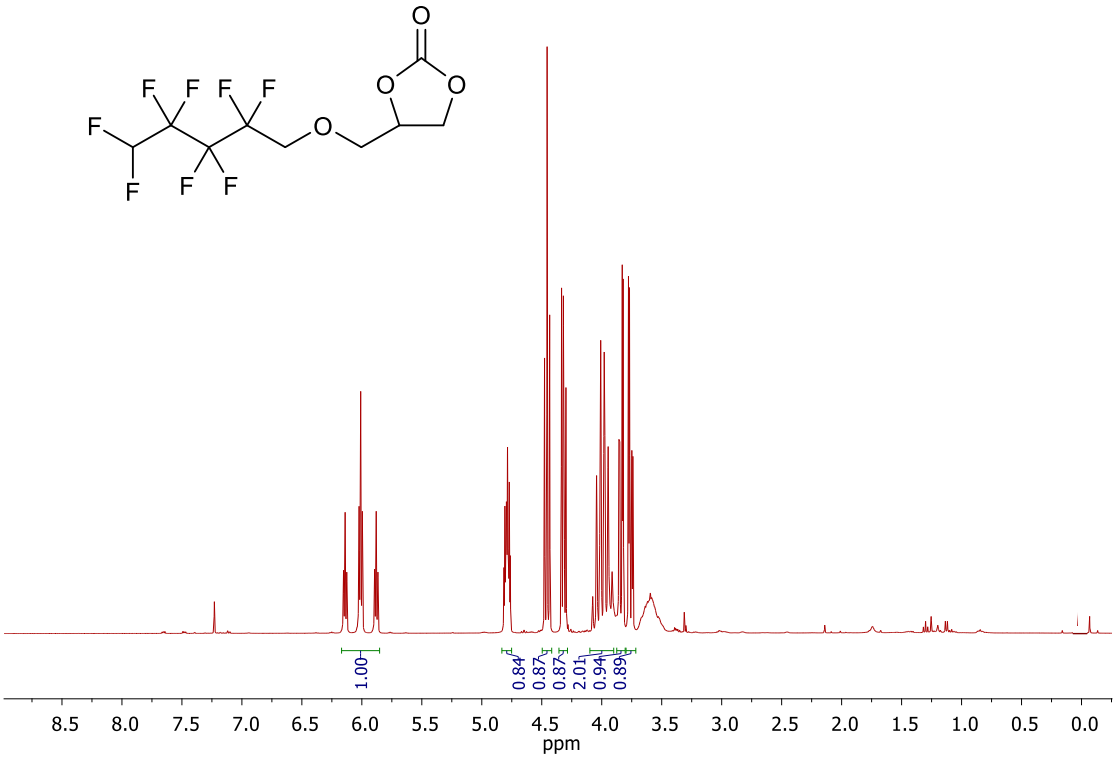

Figure S42. $^{13}C\{^{1}H\}$ NMR spectrum of 4-(((2,2,3,3,4,4,5,5-Octafluoropentyl)oxy)methyl)-1,3-dioxolan-2-one **6j** in $CDCl_3$

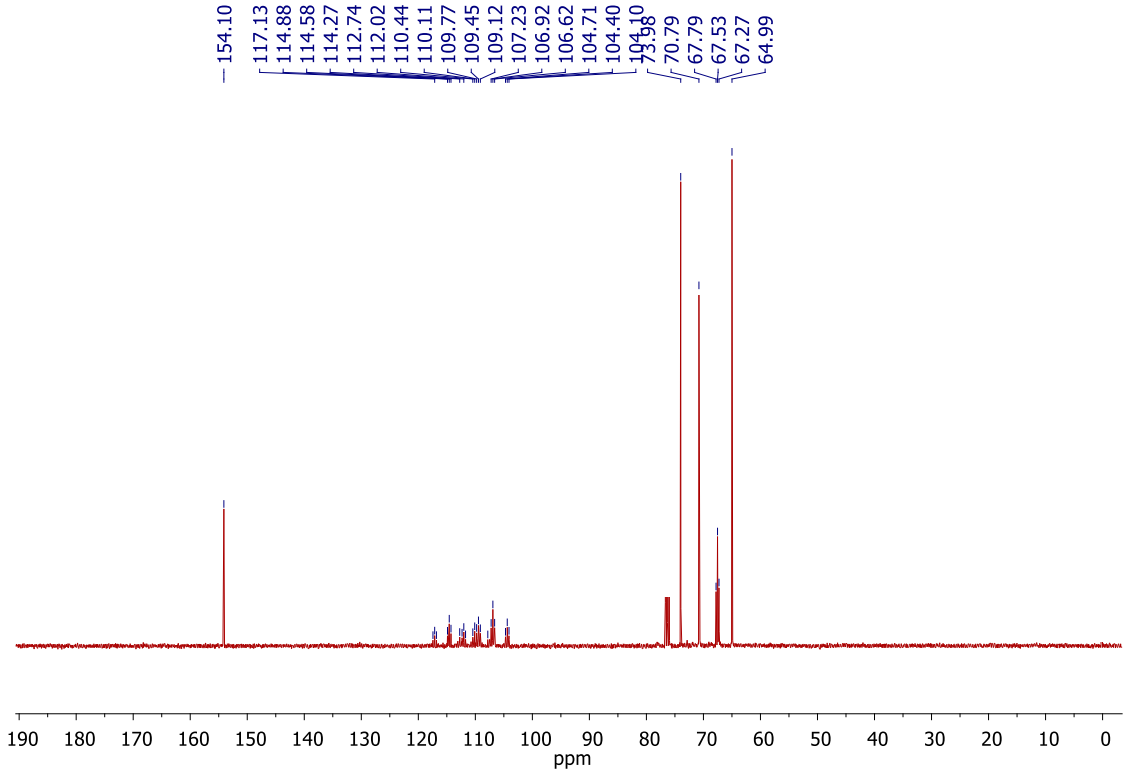

Figure S43. ^{19}F NMR spectrum of 4-(((2,2,3,3,4,4,5,5-Octafluoropentyl)oxy)methyl)-1,3-dioxolan-2-one **6j** in $CDCl_3$

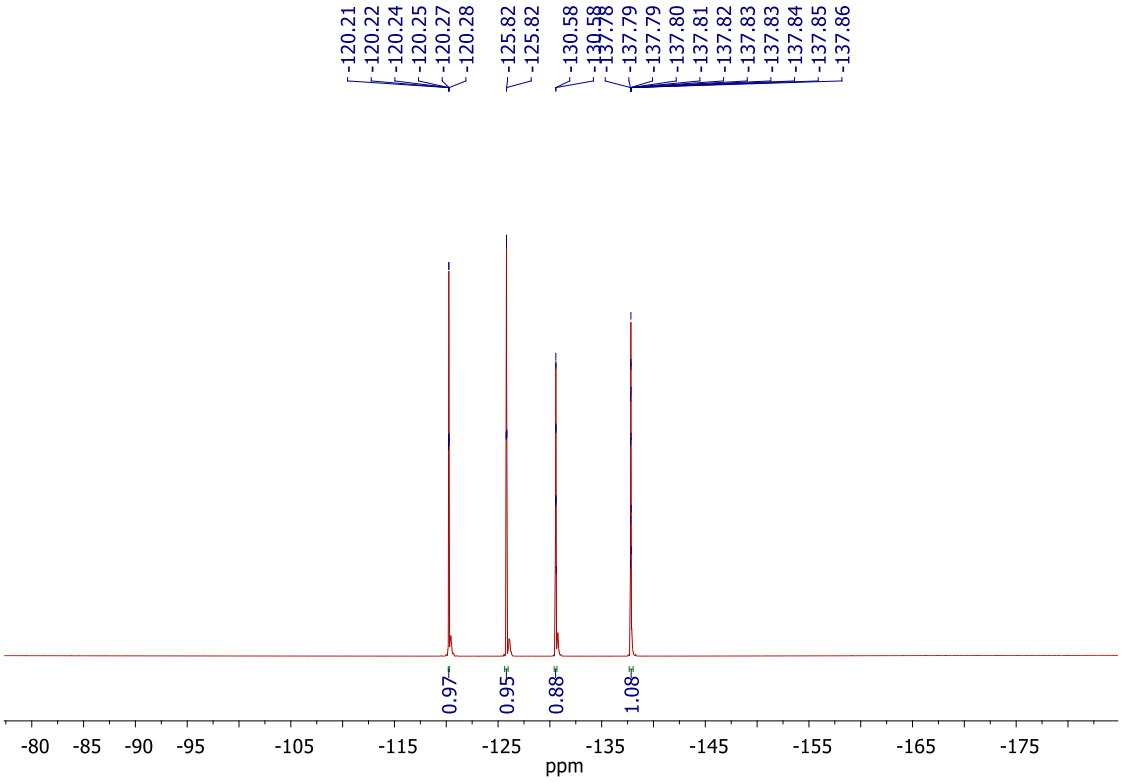

REFERENCES

[1] J. Rintjema and A. W. Kleij, *ChemSusChem*, 2017, **10**, 1274–1282.

[2] G. Fiorani, M. Stuck, C. Martín, M. M. Belmonte, E. Martin, E. C. Escudero-Adán and A. W. Kleij, *ChemSusChem*, 2016, **9**, 1304–1311.

[3] J. A. Castro-Osma, M. North and X. Wu, *Chem. Eur. J.*, 2016, **22**, 2100–2107.

[4] J. Martínez, J. A. Castro-Osma, A. Earlam, C. Alonso-Moreno, A. Otero, A. Lara-Sánchez, M. North and A. Rodríguez-Diéguez, *Chem. Eur. J.*, 2015, **21**, 9850–9862.

[5] J. Martínez, J. A. Castro-Osma, C. Alonso-Moreno, A. Rodríguez-Diéguez, M. North, A. Otero and A. Lara-Sánchez, *ChemSusChem*, 2017, **10**, 1175−1185.

[6] J. A Castro-Osma, J. Martínez, F. de la Cruz-Martínez, M. P. Caballero, J. Fernández-Baeza, J. Rodríguez-López, A. Otero, A. Lara-Sánchez and J. Tejeda, *Catal. Sci. Technol.*, 2018, **8**, 1981–1987.

[7] D. O. Meléndez, A. Lara-Sánchez, J. Martínez, X. Wu, A. Otero, J. C. Castro-Osma, M. North and R. S. Rojas, *ChemCatChem*, 2018, **10**, 2271–2277.

[8] J. Steinbauer, A. Spannenberg and T. Werner, *Green Chem.* 2017, **19**, 3769–3779.

[9] E. Feng. H. O. House and N. P. Peet, *J. Org. Chem.*, 1971, **36**, 2371–2375.

[10] R. W. W. Hooft and B. V. Nonius, *COLLECTED, Program for Collecting Data on Data on CCD Area Detectors*, **1998**, Delft, The Netherlands.

[11] Z. Otwinowski and W. Minor, *Methods Enzymol.*, 1997, **276**, 307–326.

[12] Z. Otwinowski, D. Borek, W. Majewski and W. Minor, *Acta Crystallogr*., 2003, **A59**, 228–234.

[13] G. M. Sheldrick, *Acta Cryst*., 2015, **A71**, 3–8.

[14] G. M. Sheldrick, *Acta Cryst*., 2015, **C71**, 3–8.

[15] *APEX3* (**2016**), *SAINT* (**2015**) and *SADABS* (**2015**). Bruker AXS Inc., Madison, Wisconsin, USA.

[16] *XP–Interactive molecular graphics, Version 5.1*. Bruker AXS Inc. Madison, Wisconsin, USA, **1998**.